The International Maritime Transport and Logistics (MARLOG 15) - ISSN 2974-3141
http://dx.doi.org/10.21622/MARLOG.2026.15.1.62
Smart & Resilient Logistics Corridors Future Gateway to the Green Trade

Assessing Climate Change Impacts on Potential Wave Heights and Coastal Inundation in Perth, Australia: A Numerical Modelling Approach

Mohamed M. Abouelnaser [1], Kumari Gamage [2] , and Shasha Wang [3]

(1) School of Civil Engineering, Engineering Institute of Technology, Perth Campus, Australia; 39805@student.eit.edu.au
(2) School of Civil Engineering, Engineering Institute of Technology, Brisbane Campus, Australia; kumari.gamage@eit.edu.au
(3) School of Civil Engineering, Engineering Institute of Technology, Melbourne Campus, Australia; Shasha.wang@eit.edu.au

Keywords: Climate Change Impact, Coastal Inundation, IPCC RCP / SSP Scenarios, Coastal Resilience, Numerical Modelling, Perth, Sea Level Rise

ABSTRACT

In view of the ongoing global climate changes, low-lying coastal cities of the world, including Perth in Western Australia, are encountering escalating threats from extreme wave events along with sea level rise. This research focuses on the compounding impacts of climate change on wave heights and coastal inundation forms using an integrative numerical modelling approach. Implementing high-resolution bathymetric data, 45-year offshore wave hindcasts, and IPCC AR6 sea-level rise projections across different Representative Concentration Pathways, the work has been able to simulate coastal hazard scenarios using DHI MIKE 21. The existing literature points out seasonal swell regimes and low-frequency cyclonic activity as the main drivers of Perth's vulnerability, but there are few studies that describe it risk under changing climate. This research addresses this gap by linking Extreme Value Analysis (EVA) to scenario-based modelling in order to profile significant wave characteristics and coastal flooding changes. The outcomes show that historic and future Hags differ up to 10% in the prevalence of significant wave heights across major prevailing swell directions (180°, 225°, 270°) with significant wave height overstepping 9.2 m under the extreme RCP 8.5 (SSP5-8.5) LC scenarios. Inundation footprints for Fremantle and Mullaloo back under 100-year return periods and high-emissions scenarios significantly reflect inland penetration, posing a serious threat to the coastal environment, and showcasing the importance of adaptive coastal infrastructure development and resilience planning. The study emphasizes the effectiveness of numerical methods to understand and estimate climate change through coastal interactions. Therefore, it should be considered as the basis of proactive adaptation guidelines. The results add to the ongoing academic conversation around climate-resilient urban planning and promote the enhancement of predictive skills for coastal hazard assessments under deep uncertainty.

2. INTRODUCTION

Coastal regions are the sectors which are mostly affected by the wind and wave storms flooding sea level rise, increased storm activity, and the transformation of wave climate to anthropogenic driven climate change. Consequently, Perth, Western Australia (WA), which is a city located on the changing eastern area of the Indian Ocean with narrow continental shelves and swells bringing the event of a coastal hazard. Despite the growing agreement on the global outcomes of climate change, regional assessments concerning the future coastal inundation risk, especially which considers local

http://dx.doi.org/10.21622/MARLOG.2026.15.1.62

bathymetric complexity, wave climatology, and probabilistic sea level scenarios, still needs further investigation.

The literature review in section 2 discussed the wave and storm surge regimes along the Western Australian coast and the essential factors that are responsible for them. These are the seasonal changes in wind-wave systems [1]. Earlier studies have been more concerned with large-scale climatology or used historical hindcasts without thinking about the improvement of the patterns of atmospheric teleconnections, like ENSO variability, on the trajectories of storms and on local extreme wave events [2]–[4] Moreover, only a few studies have taken into consideration the full effect of the sea level rise that is caused by different Representative Concentration Pathways (RCPs) / Shared Socioeconomic Pathways (SSPs) for Perth [5]–[13]. The research is to fill the gap through a numerical model that will have the ability to quantify future wave heights and risks of coastal inundation in Perth. The research will study the impact of climate change on significant wave heights and the risks of coastal inundation. The research is based on 45 years of offshore hindcast wave datasets and will use models of digital bathymetric and topographic data and the chain of the sea level rise which is linked to Intergovernmental Panel on Climate Change's Sixth Assessment Report IPCC AR6 (IPCC AR6) RCPs/ SSPs.

In terms of the defined approach in Section 3, the DHI MIKE 21 is employed for spectral wave modelling, a 384,000-element unstructured mesh is used for spectral wave, hydrodynamic simulation, and Weibull/Method of Moments techniques are used for Extreme Value Analysis (EVA) evaluation. The article then gives an overview of the climatic and oceanographic drivers followed by the schematic of the numerical framework. The results are demonstrated by scenario-based comparisons of the maxima of wave height and the inundation footprints, ending with the issues of coastal infrastructure and planning adaptation. Figure 1 represents the study area location of Perth, WA. Meanwhile. Figure 2 represents the numerical methodology flow chart followed for the study [14]–[17]

The motive behind this study is assessing climate change impacts on potential wave heights and coastal inundation in Perth using numerical modelling approach. Assessing climate change impacts on potential wave heights shall enhance the ability to plan of infrastructure and the implementation of the other community measures which are sensitive to the risks. As the city of Perth expands along the vulnerable shorelines, the necessity in forecasting of coastal hazards will increase as a form of an early adjustment (i.e. proactive adaptation). In particular, the modelling of future extreme weather events shall serve as a predictive tool that shall enable the identification of future coastal induction.

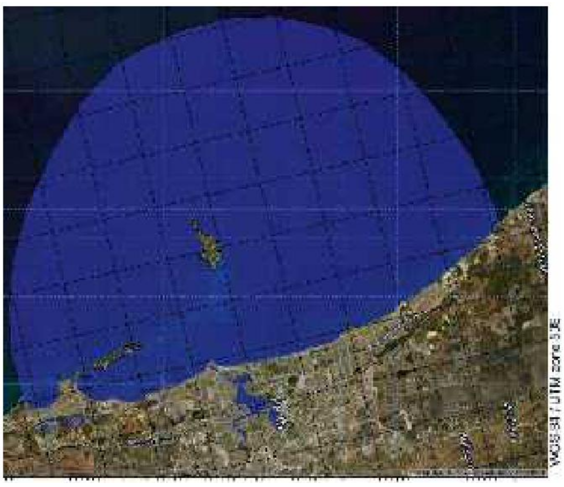

Figure 1: Study zone of Perth, WA

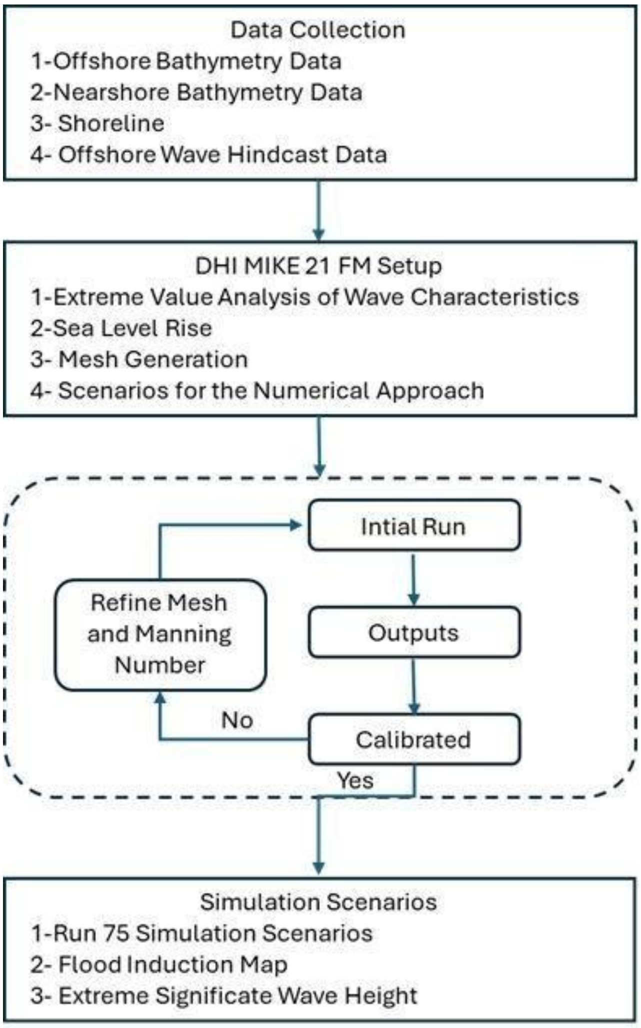

Figure 2: Numerical Methodology Flow Chart followed for the Study.

3. LITERATURE REVIEW

Australian Department of Climate Change [1] demonstrates that Perth's coastal location is influenced by its geographical position along the Indian Ocean margin and the dominant large-scale climatic systems that determine regional oceanographic and atmospheric conditions. The Southern Ocean's long- fetch swell mostly hits its shoreline, but the wave climate changes with the seasons because of mid- latitude storm systems in the austral winter and subtropical high-pressure systems in the summer (Author). The exposure to high-energy waves can change a lot during the year. For example, in the winter, the coast gets a lot of energy from stronger south-westerly swells, which are affected by storms in these latitudes [1], [18]. Perth nearshore morphology picks up signals from both persistent swell regimes and short-lived storm surges. The latter are more often caused by low-pressure systems than by tropical cyclones. The continental shelf off southwestern Australia is relatively narrow, which also affects the larger physical setting. A narrow shelf width makes it easier for offshore wave energy to move toward the shore without losing too much of it. This geomorphological feature amplifies extreme events, storm surge elevations on top of already strong swell episodes can be more dangerous where there is little frictional damping. Perth's beaches get more direct deepwater-to-shore energy transfers than broader-shelf coastal systems, which often reduce incoming wave heights through long shoaling zones. Local bathymetry can still cause strongly refracted wave fields to form, but unprotected stretches are still very exposed. Seasonal weather drivers make things even more unpredictable. The wind field along much of western Australia's coast is controlled by the interaction of subtropical ridging and short- lived frontal activity. Under current climate norms, modelling studies have discussed climate change could lead to more tropical cyclones affecting the area in the next few decades [1], [5], [19], [2], [20].

The potential arises from elevated sea surface temperatures migrating poleward, potentially prolonging the lifespan of cyclonic systems prior to dissipation. When both tidal phase and meteorological forcing reach their highest points at the same time, the co-occurrence factor can cause water levels to rise far above what is normally expected. For instance, a surge cresting during spring tide could result in disproportionately large inundation footprints in contrast to surge timing near neaps. These dynamics illustrate the rationale for incorporating joint probability analysis in hazard assessments instead of isolating individual forcings. Wave climate variability is closely linked to extensive atmospheric teleconnections that impact Australian waters. El Niño-Southern Oscillation (ENSO) [2], [21] and other oscillations change the paths of cyclones in northern basins and the amount of storminess around southern margins, especially on interannual scales. There is still debate about how ENSO shall change as the world warms, but scenarios that include changes in ENSO behaviour suggest that extreme wave events shall happen more. This could indirectly affect Perth by changing the path of storms in the region or creating strange wind patterns over the Indian Ocean. The physical makeup of the coastline is also important. Much of Perth's coastal area is sandy beaches with dune systems and rocky headlands. The direction of waves and the direction of currents are the main forces that move sediment. Depending on the angle at which waves hit, episodic reversals can move sand along the shore or out to sea [1], [5], [19], [2], [20].

Waters et al. [22] Spatial heterogeneity and changing over time are the two main expressions of cyclones that reside on Australia's coastlines, which are important for understanding the exposure of Perth. Historically, the western seaboard south of the tropics has experienced fewer direct tropical cyclone (TC) landfalls compared to northern regions, largely due to the sharp thermal gradient and cooler sea surface temperatures limiting cyclone persistence at these latitudes. Still, significant remnants of systems do sometimes move into subtropical and even temperate areas, where they can still cause damage with intense winds and rough seas. This rarity does not lessen their threat; infrequent but high- magnitude events can have effects that are out of proportion. According to studies [23]-[27] on hazard classification, coastal areas are more likely to have extreme winds than inland areas because they are more exposed to storm systems that form over open water. Simulation scenarios for Perth have shown that non-cyclonic wind hazards, which are more common in southern coastal cities, could become more stronger due to climate change [1], [5], [13], [20], [28]-[31]. Mori et al. [32] define that the increase in modeled non-cyclonic risk coincides with recent studies suggesting that specific climate change scenarios may lead to poleward shifts in tropical cyclone tracks, resulting in more frequent interactions between dissipating cyclones and southern coastlines.

Research into storm surge processes associated with tropical cyclone events demonstrates significant complexity in attributing impacts to historical occurrences [5], [32], [33], [33]-[36]. Surge vulnerability is influenced not only by storm intensity but also by track geometry, approach speed, and tidal phase alignment at landfall or the nearest passage. This means that ex-tropical systems can still cause dangerous surge conditions even if they do not have full cyclone structural system. It is crucial to acknowledge that climate model ensembles employed for evaluating historical baselines in relation to future projections possess intrinsic limitations in simulating cyclone inner-core dynamics due to resolution constraints [22]. Wind and offshore wave hindcasts tend to record multi-decadal records [5], [37]-[41].

4. METHODOLOGY AND NUMERICAL MODELLING

4.1 Bathymetry and Digital Elevation Model

Current bathymetric and Digital Elevation Models (DEM) exhibit potential yet constrained applicability for coastal management and climate change impact evaluation in Western Australia [42]- [47]. The Digital Earth Australia Coastlines datasets offer a uniform view of coastal changes across the country. Since 1988, 22% of Australia's non-rocky coastline has undergone major changes [48], [49]. Table 1 and Figure 3 summarize used Bathymetry, DEM, and shoreline data which is used to generate the model mesh dataset.

Table 1. Model's Bathymetry, DEM, and Shoreline Dataset

Data	*Dataset*
Offshore Bathymetry Data	GEBCO Dataset [42] Global Bathymetry and Topography SRTM [43] NASA SRTM Global 1 arc [44]
Nearshore Bathymetry Data	Multibeam Dataset of Australia - 50-meter Grid [46], [45] Digital Elevation Model (DEM) - 5-meter Grid [47]
Shoreline	Digital Earth Australia Coastlines [50], [51] Global Shoreline Dataset [52]

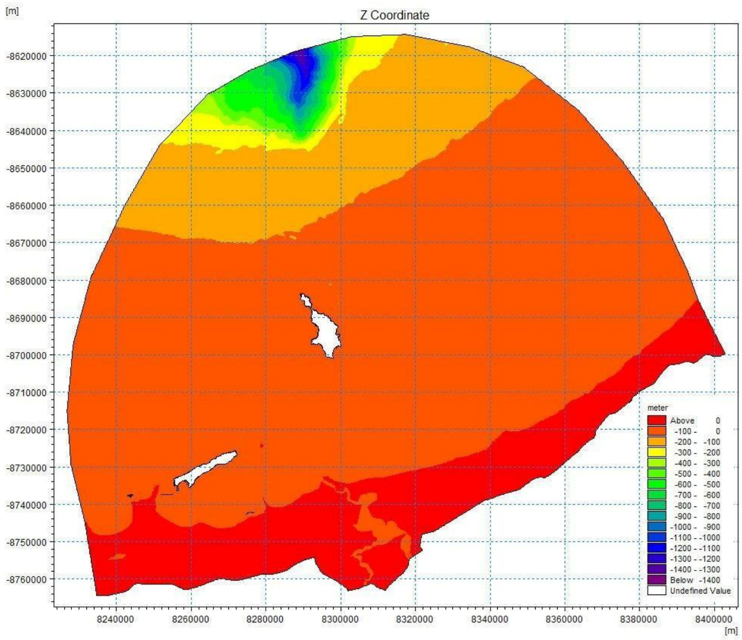

Figure 3: Bathymetry and Digital Elevation Data for Perth, WA, visualized by DHI Mike Mesh

4.2 Offshore Wave Hindcast Data of Wind-Wave Characteristics

Offshore wave hindcast datasets of wind-wave characteristics used for the model cover 45 years via two wave datasets, as defined in Table 2 [53]–[55]. In addition, Figure 4 represents the offshore dataset location.

Table 2. Offshore Wave Dataset Characteristics for Perth, WA

Data	*Dataset*	*Note*	*Start Data*	*End Data*
Wave Dataset (1)	CMEMS Dataset (1) [53], [54]	Globally validated - offshore Significant wave height Root mean square (RMS) equals to 22 cm [56]	1st January 1980	30th April 2023
Wave Dataset (2)	CMEMS Dataset (2) [55]	Globally validated - offshore Significant wave height Root mean square (RMS) equals to 2 cm [56]	1st May 2023	1st April 2025

Figure 4 represents the offshore dataset location. Meanwhile, Figure 5 and Figure 6 represent the offshore significant wave height (Hs) of wind-wave characteristics used for the model cover 45 years via two wave datasets, in accordance with Table 2 [53]–[55].

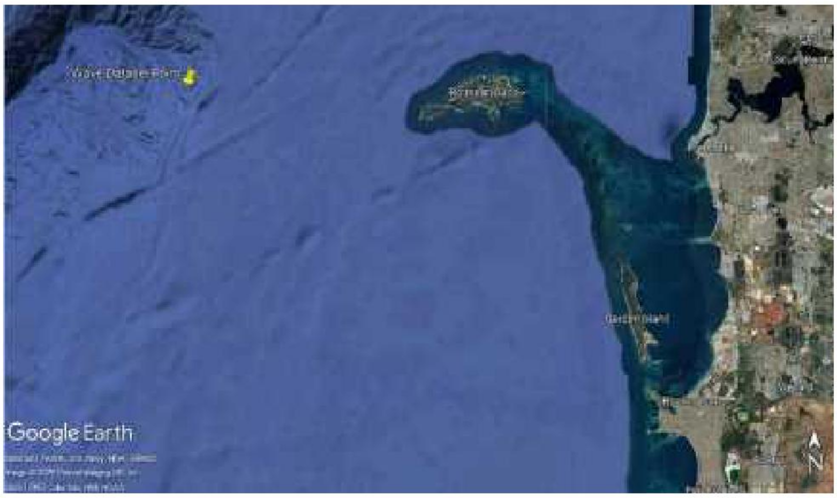

Figure 4: Offshore Dataset Point Location (Lat -32.00, Long 115.20 WGS 84) in front of Perth, WA

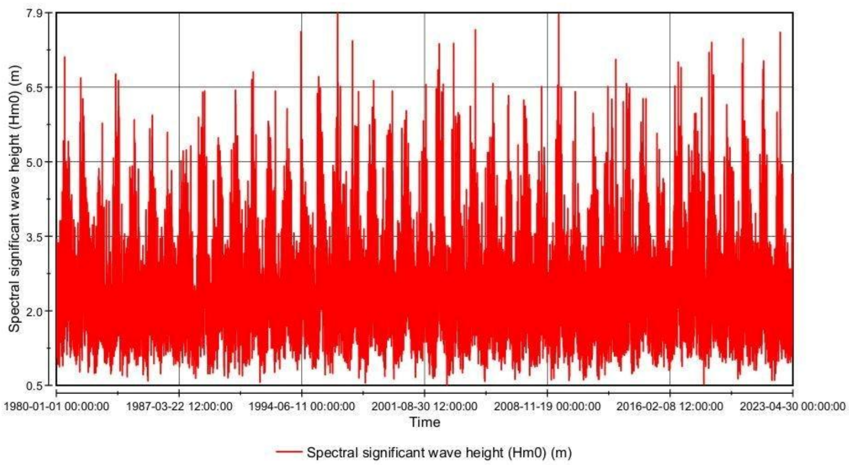

Figure 5: Wave Dataset (1) Spectral Hs, from 1980 till 2023, for the Offshore Wave of Perth, WA

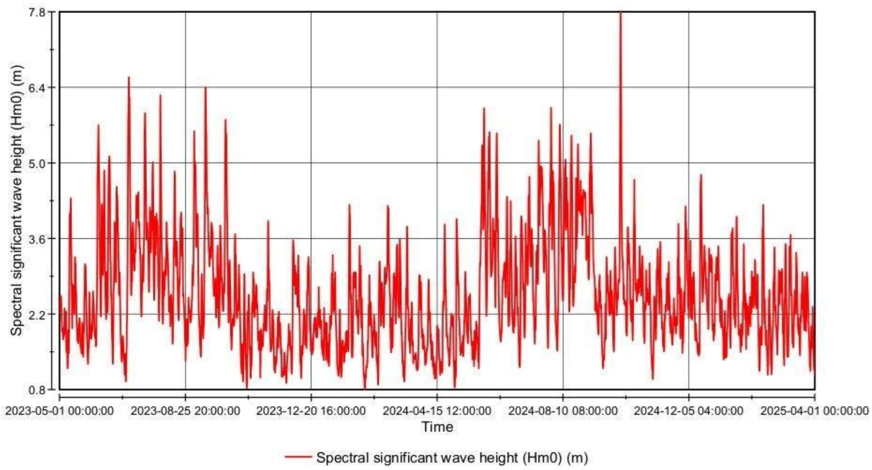

Figure 6: Wave Dataset (2) Spectral Hs, from 2023 till 2025, for the Offshore Wave of Perth, WA

The hindcast data suggests a primarily bi-directional wave climate with over 95% of the significant wave heights blowing from the southwest (225°) and the west (270°) directions. This bi-directional precedence has crucial effects on coastal structure design, harbour orientation, and beach erosion assessments since it represents the highly energetic sea states that have an impact on the area. For coverage over 99% of the significant wave heights, the direction 180°, 225° and 270° shall be used for EVA, as presented in Figure 7 and Table 3.

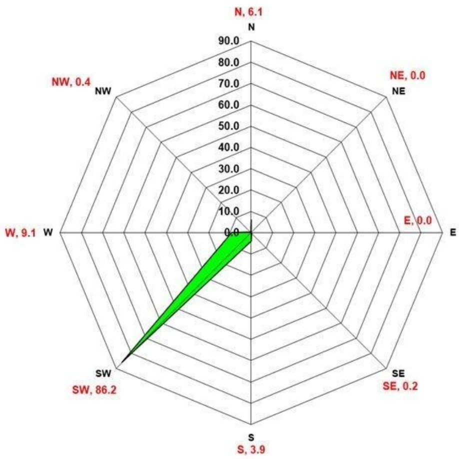

Figure 7: Coverage Percentage for Different Directions, from 2023 till 2025, for Wave Dataset of Perth, WA

Table 3. Dataset Coverage Percentage for Different Directions

Direction (Degree)	*Percentage (%)*
0 °	0.06
45 °	0.03
90 °	0.04
135 °	0.22
180 °	3.92
225 °	86.19
270 °	9.11
315 °	0.43

To investigate EVA for Perth and the climate change impact of the significant Hs, the EVA is estimated for two scenarios. The first scenario covers EVA for direction 180°, 225° and 270°, from 1980 till 2025. Meanwhile, the second scenario covers the same directions for Perth, from 1980 till 2001, as defined in Table 4. As illustrated by Lucio et al. [57], the comparison between both scenarios with different return periods can illustrate the impact of the climate change to the estimated storm significate Hs.

Table 4. EVA Scenarios for Perth, WA

Scenarios	*Coverage*	*Length*	*Source*
Scenario (1)	from 1980 till 2025	≈45 years	[53], [55]
Scenario (2)	from 1980 till 2001	≈21 years	[53], [55]

4.3 Extreme Value Analysis of Wind-Wave Characteristics

Eextreme value Analysis (EVA) methodology in coastal field is an adequate statistical distance for measuring extreme situations and events based on the obtained meteorological data for the low- probability occurrence of extreme coastal events would be [15], [58]. The alteration of extreme wave height events around Perth and other regions off the open sea over the past years is ascribed to the fact that they are affected mainly by natural cycles and human-induced changes in the atmosphere and oceans. Seasonal climatology has been the principal influence on wave patterns, with winter months frequently displaying fast increments in wave heights and peak values occurring in December and January [59]. For instance, ENSO phases can reverse the routes of storms or the direction of the winds over the Indian Ocean. This would, in turn, modify how the waves would be advancing to the coasts of Perth. Technical forecasting based on the datasets of both hindcast and reanalysis indicate that a maximum nearshore level can be physically limited by the depth restriction of the area [2]–[4].

For this study, a proposed approach of Weibull/Method of Moments is used for EVA, as the estimated best fit curve method [60]. In accordance with Scenario (1), Table 5 summarizes the estimated EVA curve parameters of Weibull Distribution using Method of Moments of the offshore Hs blowing from direction 180°, 225° and 270°.

Table 5. EVA Parameters of Weibull Distribution using Method of Moments of the Offshore Hs blowing from Direction 180°, 225° and 270°, from 1980 till 2025, for Perth, WA

Direction (Degree)	*180 °*	*225 °*	*270 °*
Weibull/Method of Moments PPCC	0.995	0.998	1.000
Location Parameter	0.957	1.144	0.708
Scale Parameter	0.849	1.284	2.658
Shape Parameter	1.746	1.424	2.008

Table 6 summarizes the estimated EVA values of the offshore Hs blowing from Direction 180°, 225° and 270°, from 1980 till 2025, for Perth, WA. In addition, Figure 8, Figure 9 and Figure 10 illustrate the offshore scenario (1) Hs for different return periods (R. P) blowing from Direction 180°, 225° and 270°, respectively.

Table 6. EVA of the offshore Hs blowing from Direction 180°, 225° and 270°, from 1980 till 2025, for Perth

Direction (Degree)	H_s *1-year R. P (m)*	T_p *1-year R. P (s)*	H_s *5-year R. P (m)*	T_p *5 -year R. P (s)*	H_s *20-year R. P (m)*	T_p *20-year R. P (s)*	H_s *50-year R. P (m)*	T_p *50-year R. P (s)*	H_s *100-year R. P (m)*	T_p *100-year R. P (s)*
180 °	3.02	13.81	3.42	14.03	3.65	14.15	3.85	14.25	4.02	14.33
225 °	6.52	15.26	7.40	15.51	8.00	15.67	8.40	15.77	8.70	15.84
270 °	7.00	15.40	7.75	15.61	8.45	15.78	8.85	15.88	9.20	15.96

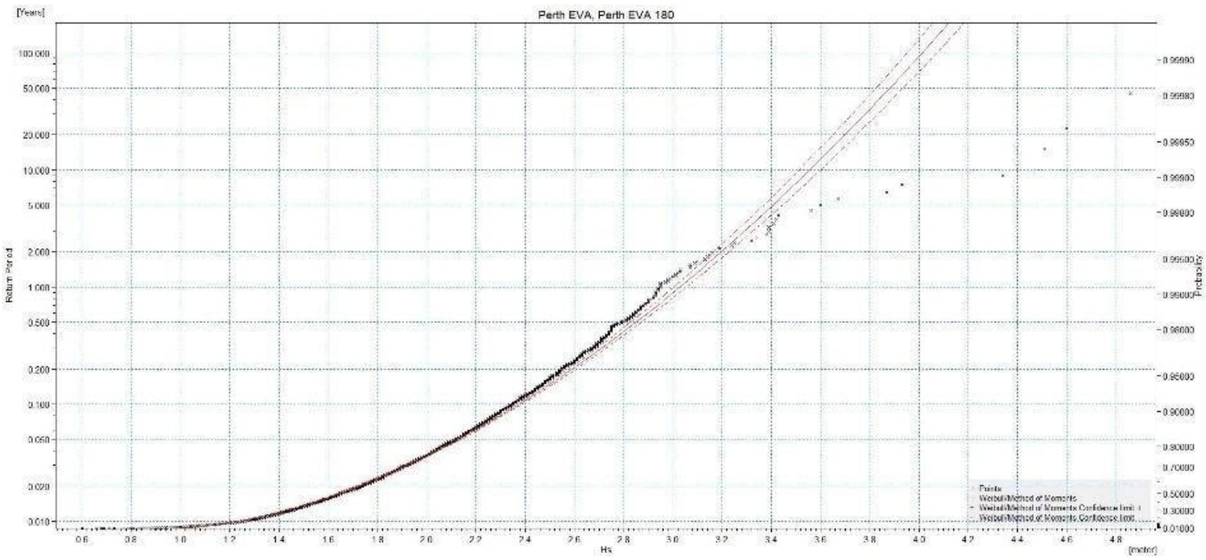

Figure 8: EVA of the Offshore Hs blowing from Direction 180 °, from 1980 till 2025.

http://dx.doi.org/10.21622/MARLOG.2026.15.1.62

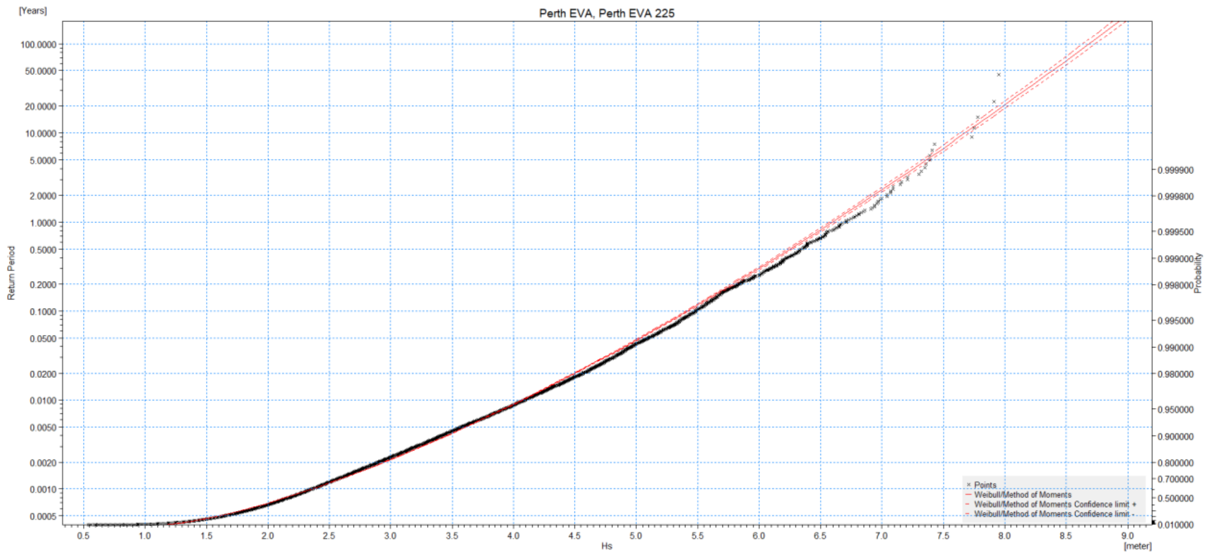

Figure 9: EVA of the Offshore Hs blowing from Direction 225 °, from 1980 till 2025.

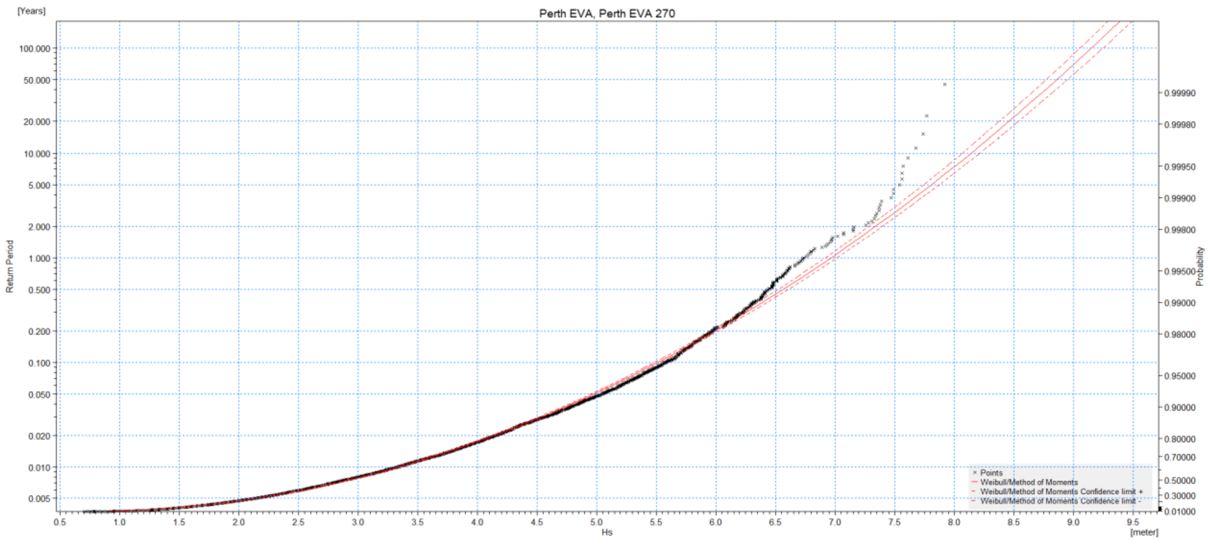

Figure 10: EVA of the Offshore Hs blowing from Direction 270 °, from 1980 till 2025.

Figure 11, Figure 12 and Figure 13 illustrate the offshore scenario (2) Hs blowing from Direction 180°, 225° and 270°, respectively.

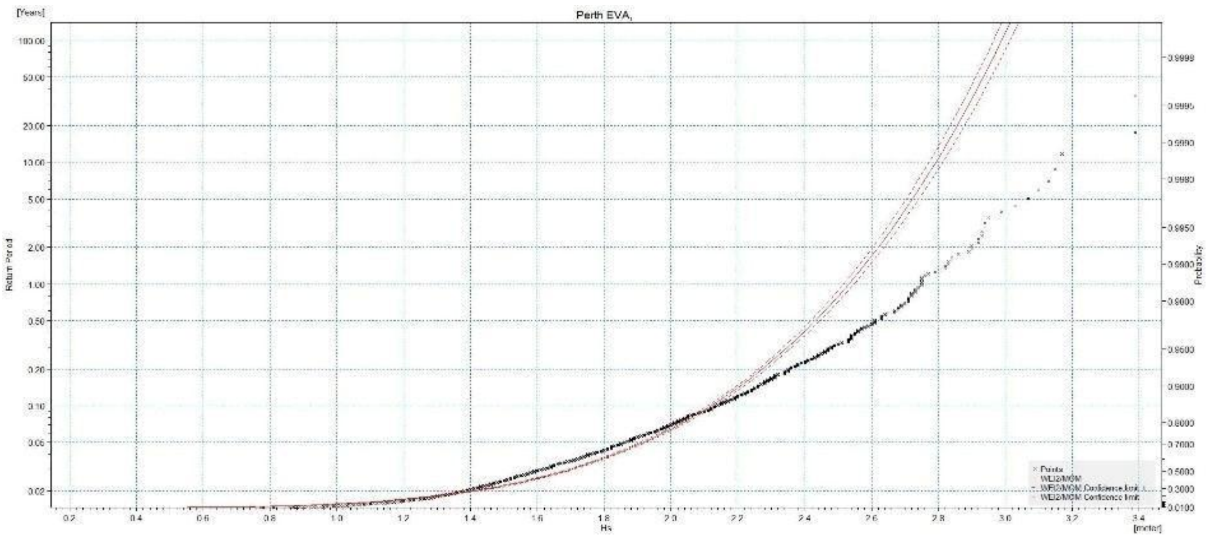

Figure 11: Extreme Value Analysis of the Offshore Hs blowing from Direction 180 °, from 1980 till 2001.

http://dx.doi.org/10.21622/MARLOG.2026.15.1.62

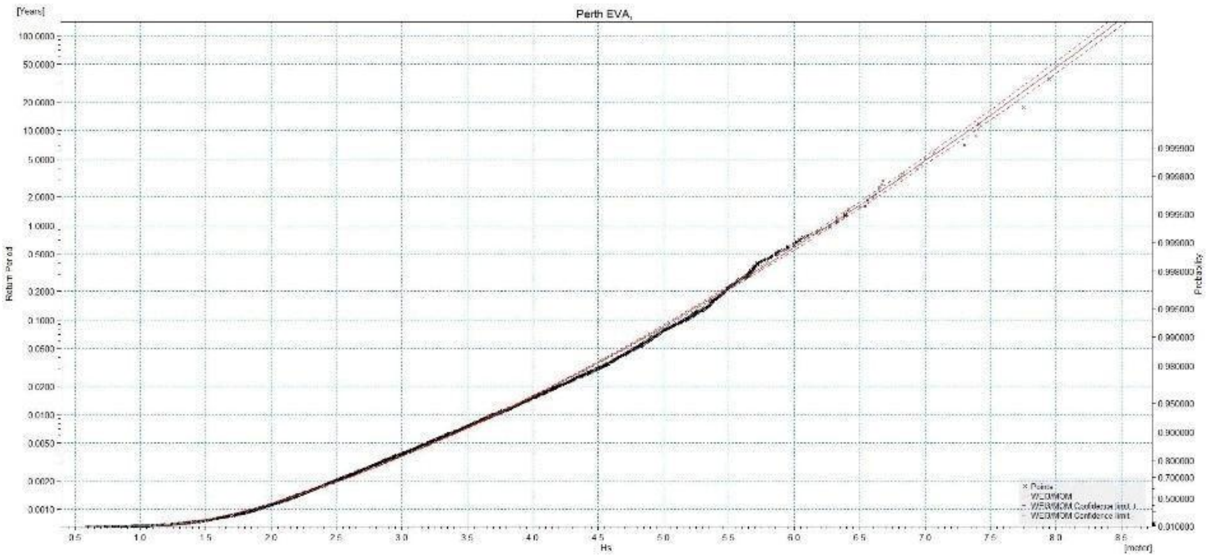

Figure 12: Extreme Value Analysis of the Offshore Hs blowing from Direction 225 °, from 1980 till 2001.

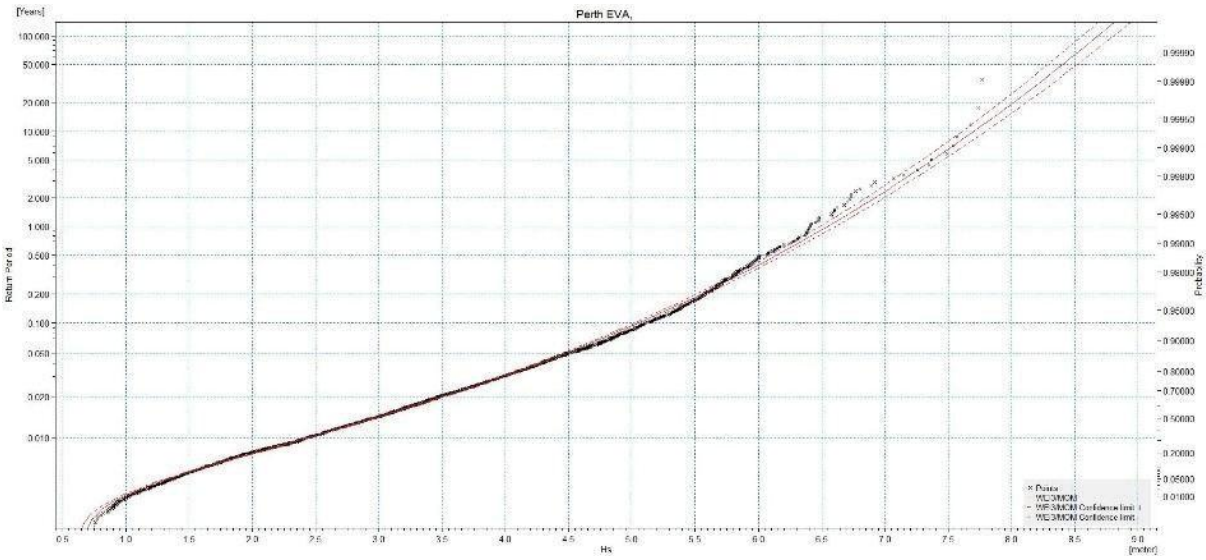

Figure 13: Extreme Value Analysis of the Offshore Hs blowing from Direction 270 °, from 1980 till 2001.

4.4 Sea Level Rise

Sea level rise (SLR) is one of the most important things that happen in the world because of climate change. SLR is the result of the sea water becoming warmer, the glaciers and the ice sheets melting, the changes in terrestrial water storage. These things are risking the integrity of infrastructure, the wellbeing of the ecosystem, and the safety of residents in more coastal cities where flooding, erosion, and seawater intrusion are the main problems. Perth is a place of extreme importance since it has exceptional oceanographic conditions and a vigorous sea breeze system, as well as a complicated coastal line geomorphology, all of which directly affect the local sea level rise consequences. Making sure that the sea level rise forecasts for Perth are correct is extremely important for the regional adaptation planning, infrastructure resilience, and risk management, especially because the temperature projections that go

as far ahead as 2130 introduce substantial uncertainties in the climate forcing, ice sheet dynamics, and local land movement [12], [61]–[63]

In Perth, the sea level rise is predicted by 2130 to range from over a meter to above 4 meters along the course of high emissions rising to multi-meters in the extreme case with possible instability in the Antarctic ice sheet. Vertical land motion and coastal geomorphology are hypothesis to have a bad influence on this situation; yet this process remains hindered in large by the ice sheet dynamics and local land subsidence or uplift effects [12], [26], [34], [64]–[68]. Representative Concentration Pathways (RCPs) / Shared Socioeconomic Pathways (SSPs) show how the amount of greenhouse gases in the air changes over time. There are different levels of radiative forcing for each one, from RCP2.6/ SSP1-2.6, which means a significant amount of mitigation, to RCP8.5/ SSP5-8.5, which means a significant quantity of emissions [6], [69]–[71].

For this study, 5 main RCPs/SSPs have been used to numerically investigate the impact of the climate change and SLR of coastal flood for Perth. Intergovernmental Panel on Climate Change's Sixth Assessment Report IPCC AR6 is used to estimate the SLR Projections for the different scenarios of RCPs/SSPs in the study, as defined in Table 7 and Figure 14 [7]–[9]. The numerical study shall be limited to the IPCC AR6 SLR values that covers the statistical quantile of 95%.

Table 7. IPCC RCPs/SSPs Scenarios and Relevant SLR used for the Study.

Scenario(s) [7]–[9]	*Statistical Quantile (%)*	*2030 (m)*	*2040 (m)*	*2050 (m)*	*2060 (m)*	*2070 (m)*	*2080 (m)*	*2090 (m)*	*2100 (m)*	*2110 (m)*	*2120 (m)*	*2130 (m)*
RCP 2.6 / SSP1-2.6 MC	50	0.09	0.14	0.20	0.25	0.31	0.37	0.43	0.50	0.58	0.64	0.69
RCP 2.6 / SSP1-2.6 MC	95	0.19	0.26	0.35	0.44	0.54	0.65	0.76	0.91	1.05	1.17	1.28
RCP 4.5 / SSP2-4.5 MC	50	0.09	0.14	0.21	0.27	0.35	0.43	0.50	0.59	0.68	0.76	0.84
RCP 4.5 / SSP2-4.5 MC	95	0.18	0.26	0.36	0.46	0.59	0.73	0.87	1.04	1.20	1.35	1.50
RCP 7.0 / SSP3-7.0 MC	50	0.10	0.15	0.22	0.29	0.38	0.47	0.58	0.70	0.79	0.90	1.01
RCP 7.0 / SSP3-7.0 MC	95	0.18	0.25	0.37	0.49	0.62	0.79	0.98	1.22	1.40	1.61	1.82
RCP 8.5 / SSP5-8.5 MC	50	0.10	0.16	0.24	0.31	0.41	0.52	0.64	0.79	0.89	1.02	1.14
RCP 8.5 / SSP5-8.5 MC	95	0.18	0.29	0.40	0.53	0.69	0.88	1.08	1.35	1.59	1.82	2.05
RCP 8.5 / SSP5-8.5 LC	50	0.10	0.17	0.25	0.33	0.44	0.57	0.72	0.92	1.09	1.30	1.53
RCP 8.5 / SSP5-8.5 LC	95	0.22	0.39	0.58	0.82	1.12	1.48	1.90	2.41	2.97	3.59	4.22

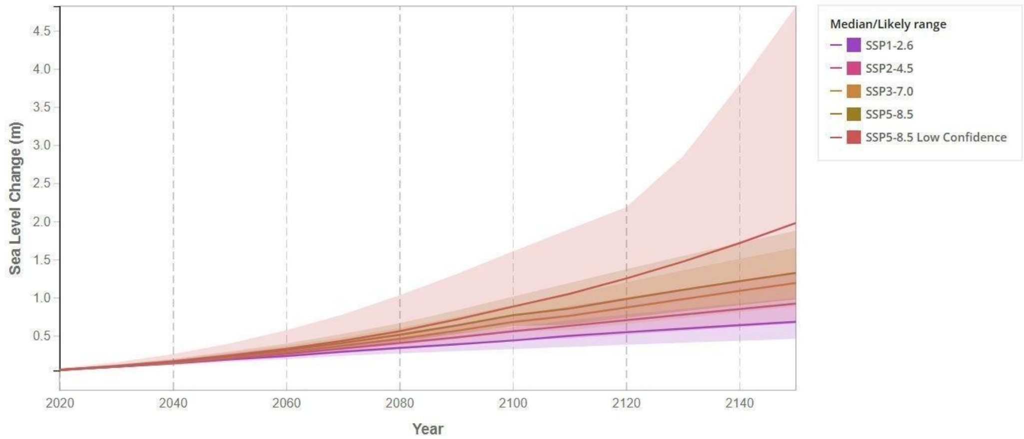

Figure 14: IPCC RCPs / SSPs Scenarios and Relevant SLR, till 2150

http://dx.doi.org/10.21622/MARLOG.2026.15.1.62

4.5 Mesh Generation and Model Calibration

Mesh. Bathymetric modelling is crucial step for numerical investigation in coastal engineering, marine science, and environmental management [72], [73]. DHI MIKE 21 is a well-known set of programs for modelling coastal and marine environments [14], [16], [17]. The most effective methods to generate meshes for making accurate bathymetric models in DHI MIKE 21 are automated unstructured mesh generation with integrated shoreline approximation and adaptive mesh refining. Optimizing mesh gradation can greatly improve accuracy while lowering processing needs [14], [16], [17], [74]. For this Study, 384,022 elements with 193,593 nodes have been used for mesh generation with global map projection of WGS 84 / UTM Zone 50. Figure 15 illustrates the generated numerical mesh, including the bathymetry and DEM datasets defined in Table 1, for Perth, WA. Meanwhile, Figure 16 illustrates the zoomed generated numerical mesh, for Fremantle and Swan River, Perth.

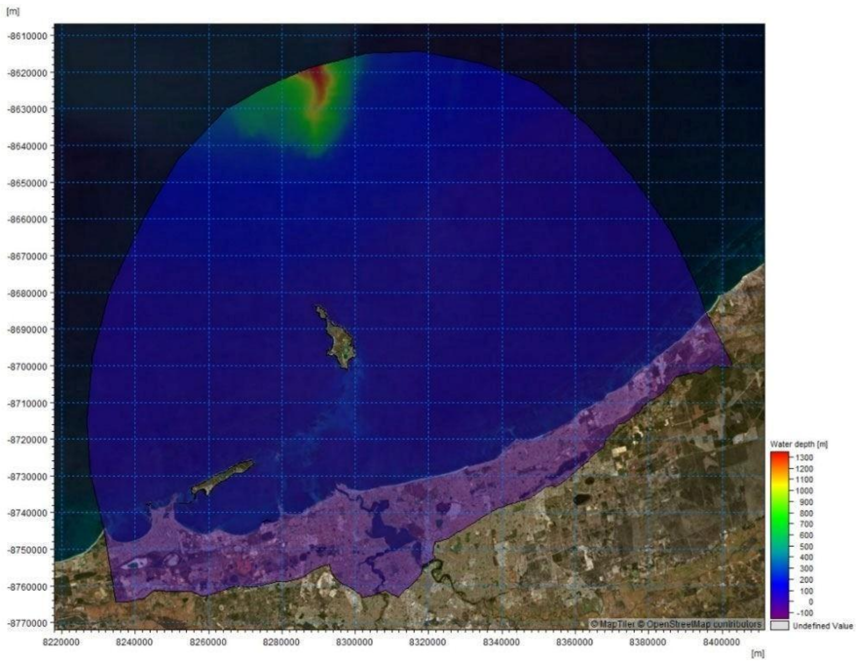

Figure 15: Generated Numerical Mesh, including the Bathymetry and DEM datasets, for Perth, WA

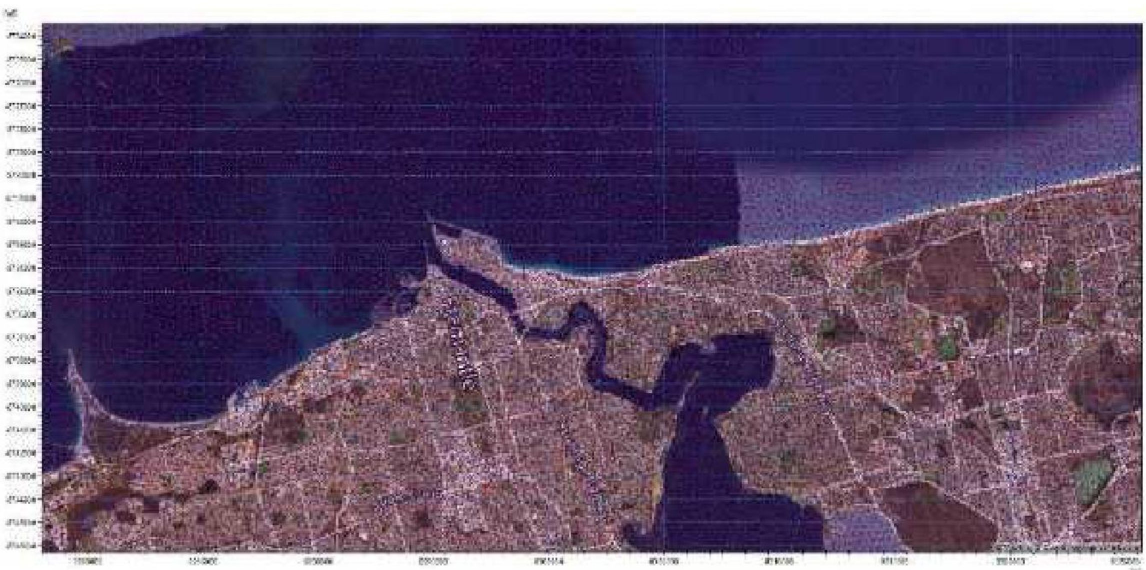

Figure 16: Mesh for Fremantle and Swan River, Perth, WA

The model is calibrated using comparison of simulated significant wave height for the basin from 3:00 AM June 1st, 2025, till 19:00 AM June 2nd, 2025. Integrated Marine Observing System (IMOS) Hillarys buoy [75], located at Lat - 31.852°, Long 115.647° WGS 84, is used for the calibration. The average difference and maximum difference between the simulated Hs and the recorded Hs by Hillarys buoy are 2 cm and 23 cm, respectively. Figure 17 shows the difference between the simulated Hsand the recorded Hs by Hillarys buoy.

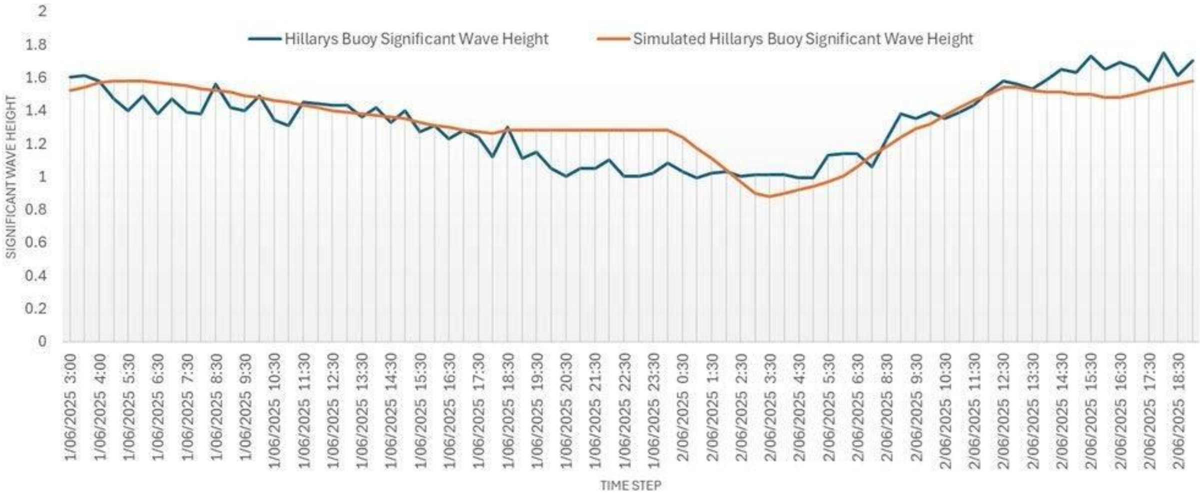

Figure 17: Simulated Hs and the recorded Hs by Hillarys buoy, located at Lat - 31.852°, Long 115.647° WGS 84

4.5 Scenarios for the Numerical Approach

For this study, 75 Scenarios are simulated to numerically investigate interaction of the main directions of extreme events, different return period and IPCC RCP / SSPs SLR, as illustrated in Figure 18 and Appendix (1).

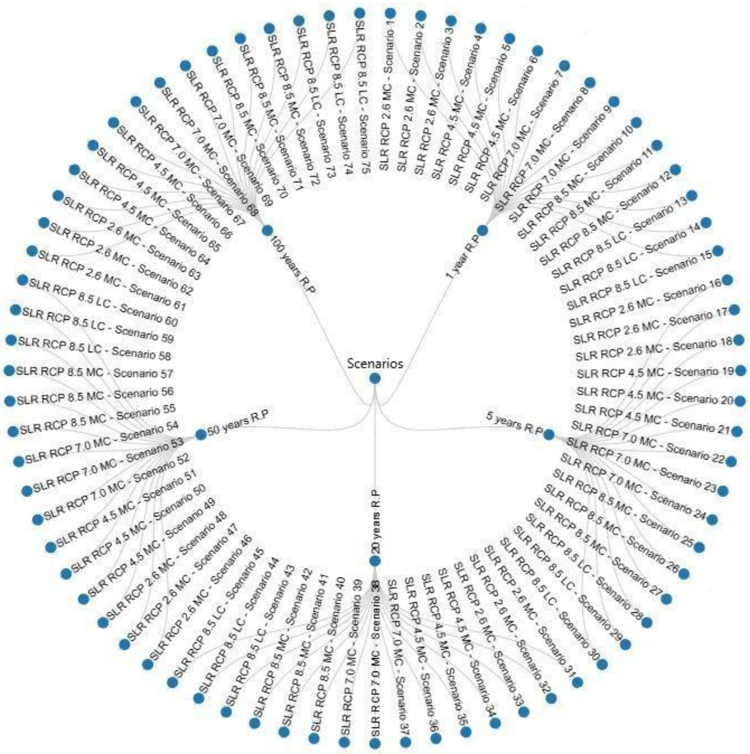

Figure 18: Main Parameters for the Simulated Scenarios

The International Maritime Transport and Logistics (MARLOG 15) - ISSN 2974-3141
http://dx.doi.org/10.21622/MARLOG.2026.15.1.62
Smart & Resilient Logistics Corridors Future Gateway to the Green Trade

5. RESULTS AND DISCUSSION

The long coastline of Western Australia is a platform for the effects of a wide range of oceanic and atmospheric drivers, thereby forming its wave climate, especially in the course of storm events. The knowledge of the change in climate of how the wave heights will increase during storms is vital for the coastal risk management, for the infrastructure planning, and for the ecosystem to be resilient. The study combines literature searches, IPCC RCP / SSP model projections, and numerical simulations. It is the beginning of a merging of the research initiatives of the theoretical and the practical, describing briefly the existing gaps and suggesting pathways into the future.

Atmospheric circulation patterns that are responsible for storm tracks and potential changes in storm intensities will be affected by the climate changes, which in turn leads to the change in wave-generating mechanisms. It is worth mentioning that these ocean waves are also modified due to their interaction with local bathymetric features which are mainly responsible for the enhancement or modulation.

In Western Australia, Hs for sea waves presents a remarkable seasonal variation whereby the value is at the peak during the winter storms which are associated with mid-latitude depressions, and it is at a minimum during the summer sea breezes. Cyclone-induced significant wave heights (Hs >3 m) reach the annual average of about 30 cases, with the highest occurrence of those averaging in July. Perth offshore wave finding shows that during severe winter storms, significant wave height can get to return period estimations of 7.0 meters (1-year) and 9.20 meters (100-year). It is worth noting Hs, which are resulting from the intersection of waves blowing from direction 270° and RCP / SSP 8.5 LC, are the maximum generated wave heights for different return periods. Table 8 summarize the comparison between both scenarios illustrates the increment percentage due to the impact of climate change to the estimated storm significate Hs, in accordance with Table 4. There is an estimated average increment percentage of 10%, 5% and 6% for the directions of 180°, 225° and 270°, respectively.

Table 8. EVA of the offshore Hs blowing from Direction 180°, 225° and 270°, for 2 scenarios, for Perth, WA

	Scenario (1), from 1980 till 2025					*Scenario (2), from 1980 till 2001*					*Increment Percentage*				
Direction (Degree)	H_s *1-year R. P (m)*	H_s *5-year R. P (m)*	H_s *20-year R. P (m)*	H_s *50-year R. P (m)*	H_s *100-year R. P (m)*	H_s *1-year R. P (m)*	H_s *5-year R. P (m)*	H_s *20-year R. P (m)*	H_s *50-year R. P (m)*	H_s *100-year R. P (m)*	*1 year R. P*	*5 years R. P*	*20 years R. P*	*50 years R. P*	*100 years R. P*
180 °	3.02	3.42	3.65	3.85	4.02	2.75	3.1	3.34	3.5	3.62	9.82%	10.32%	9.28%	10.00%	11.05%
225 °	6.52	7.4	8	8.4	8.7	6.32	6.95	7.61	8	8.4	3.16%	6.47%	5.12%	5.00%	3.57%
270 °	7.00	7.75	8.45	8.85	9.2	6.51	7.32	8.04	8.4	8.7	7.53%	5.87%	5.10%	5.36%	5.75%

Figure 19 shows the Wave Height at the entrance of Fremantle Harbour, Perth, for different SLR, Directions and R. P scenarios as defined in accordance with Figure 18 and Appendix (1). Meanwhile, Figure 20 illustrates the Hs values for different return periods. Moreover, Perth is the one of the most affected cities in the Western Australia due to the changes caused by climate and the affected population. The major factors causing these alterations are SLR and the increment in both the number of storms and their strength, as defined in table 8. Urban areas close to the coast of Perth are supposed to be faced with significant problems that arise as a result of the climate impact on coastal inundations. Proactive action strategies such as the infrastructure modernization, and proper governance, and coastal risk investigation using numerical modelling approaches may help the community to have a stable and strong coastal communities. It is expected that the coastal flooded area shall exceed ninety-seven km2 due to the extreme wave events for RCP/ SSP 8.5 LC. Figure 21 and Figure 22 illustrate the predicted flooded footprint due to extreme wave events blowing from direction 270° with SLR RCP/ SSP 8.5 LC for Fremantle and Mullaloo zone, respectively.

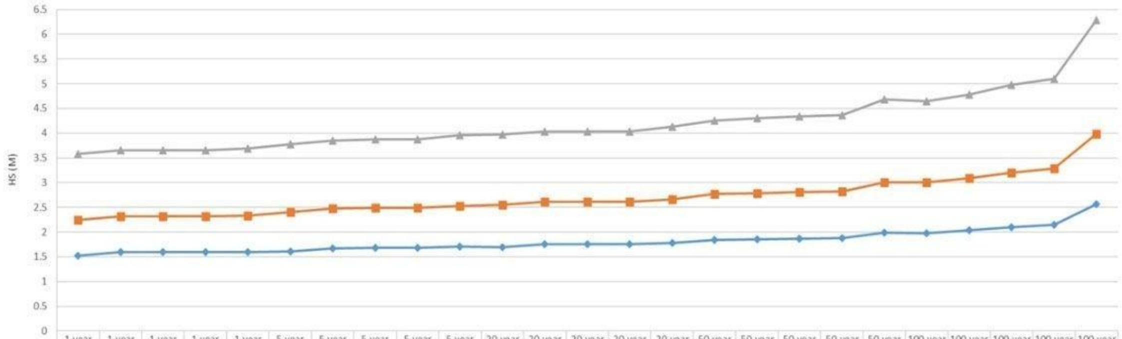

	1-year R.P - SLR RCP 2.6 MC	1-year R.P - SLR RCP 4.5 MC	1-year R.P - SLR RCP 7.0 MC	1-year R.P - SLR RCP 8.5 MC	1-year R.P - SLR RCP 8.5 LC	5-year R.P - SLR RCP 2.6 MC	5-year R.P - SLR RCP 4.5 MC	5-year R.P - SLR RCP 7.0 MC	5-year R.P - SLR RCP 8.5 MC	5-year R.P - SLR RCP 8.5 LC	20-year R.P - SLR RCP 2.6 MC	20-year R.P - SLR RCP 4.5 MC
Hs (Dir 270 Deg)	1.3387	1.3399	1.3388	1.3388	1.3571	1.3708	1.3760	1.3875	1.3847	1.4291	1.4239	1.4207
Hs (Dir 225 Deg)	0.7202	0.7255	0.7258	0.7260	0.7309	0.7985	0.8031	0.8071	0.8064	0.8252	0.8569	0.8571
Hs (Dir 180 Deg)	1.5201	1.59381	1.59389	1.59404	1.59984	1.6063	1.67076	1.68267	1.67907	1.70791	1.69722	1.75172

	20-year R.P - SLR RCP 7.0 MC	20-year R.P - SLR RCP 8.5 MC	20-year R.P - SLR RCP 8.5 LC	50-year R.P - SLR RCP 2.6 MC	50-year R.P - SLR RCP 4.5 MC	50-year R.P - SLR RCP 7.0 MC	50-year R.P - SLR RCP 8.5 MC	50-year R.P - SLR RCP 8.5 LC	100-year R.P - SLR RCP 2.6 MC	100-year R.P - SLR RCP 4.5 MC	100-year R.P - SLR RCP 7.0 MC	100-year R.P - SLR RCP 8.5 MC	100-year R.P - SLR RCP 8.5 LC
Hs (Dir 270 Deg)	1.4203	1.4233	1.4662	1.48425	1.51164	1.53245	1.53805	1.67624	1.64371	1.68889	1.76837	1.81453	2.30143
Hs (Dir 225 Deg)	0.8577	0.8591	0.8781	0.92312	0.933281	0.943539	0.947502	1.0243	1.03392	1.06164	1.10813	1.1356	1.41436
Hs (Dir 180 Deg)	1.75288	1.75561	1.78348	1.843912	1.85372	1.86358	1.87747	1.98503	1.9743	2.03448	2.09867	2.14633	2.57002

Figure 19: Wave Height at the entrance of Fremantle Harbour, Perth (Location: Latitude -32.056, Longitude-115.725. WGS 84)

http://dx.doi.org/10.21622/MARLOG.2026.15.1.62

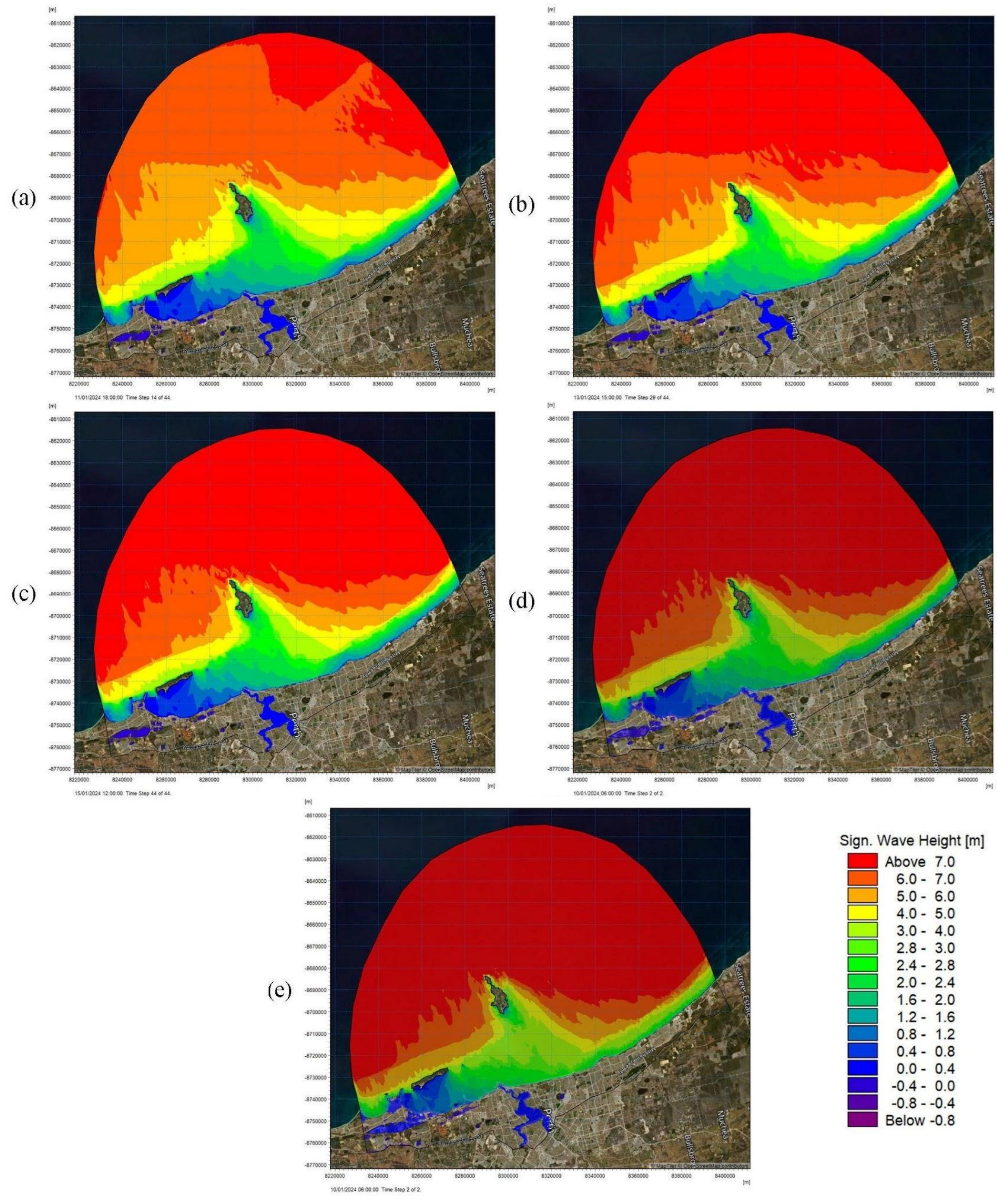

Figure 20: Highest Wave Amplitude of direction 270° with SLR RCP / SSP 8.5 LC for Perth (a) Hs for 1-year R.P, (b) Hs for 5-year R.P, (c) Hs for 20-year R.P, (d) Hs for 50-year R.P, (e) Hs for 100-year R.P

http://dx.doi.org/10.21622/MARLOG.2026.15.1.62

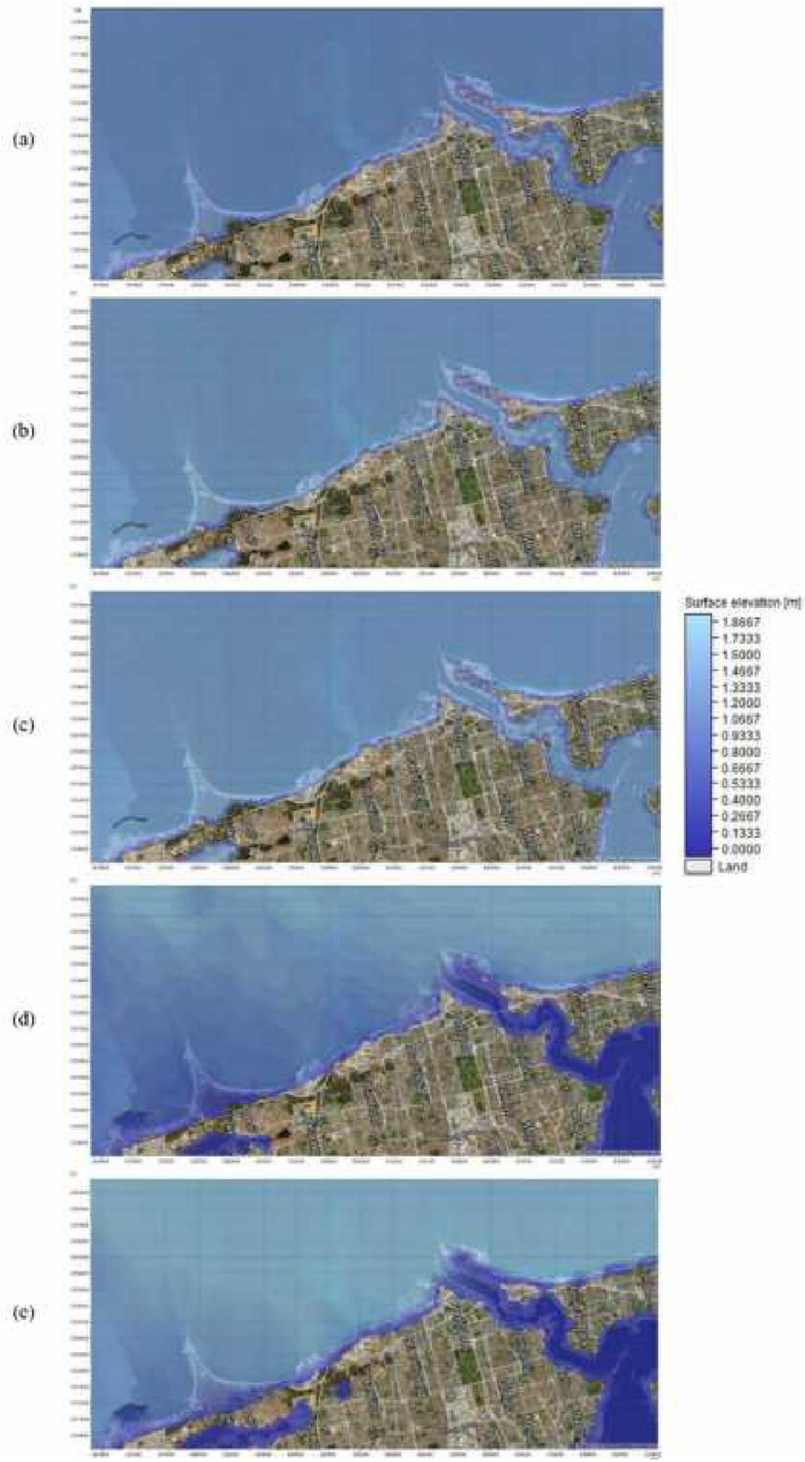

Figure 21: Flooded Footprint due to extreme Wave Events blowing from direction 270° with SLR RCP / SSP 8.5 LC for Fremantle, Perth (a) Hs for 1-year R.P, (b) Hs for 5-year R.P, (c) Hs for 20-year R.P, (d) Hs for 50-year R.P, (e) Hs for 100-year R.P

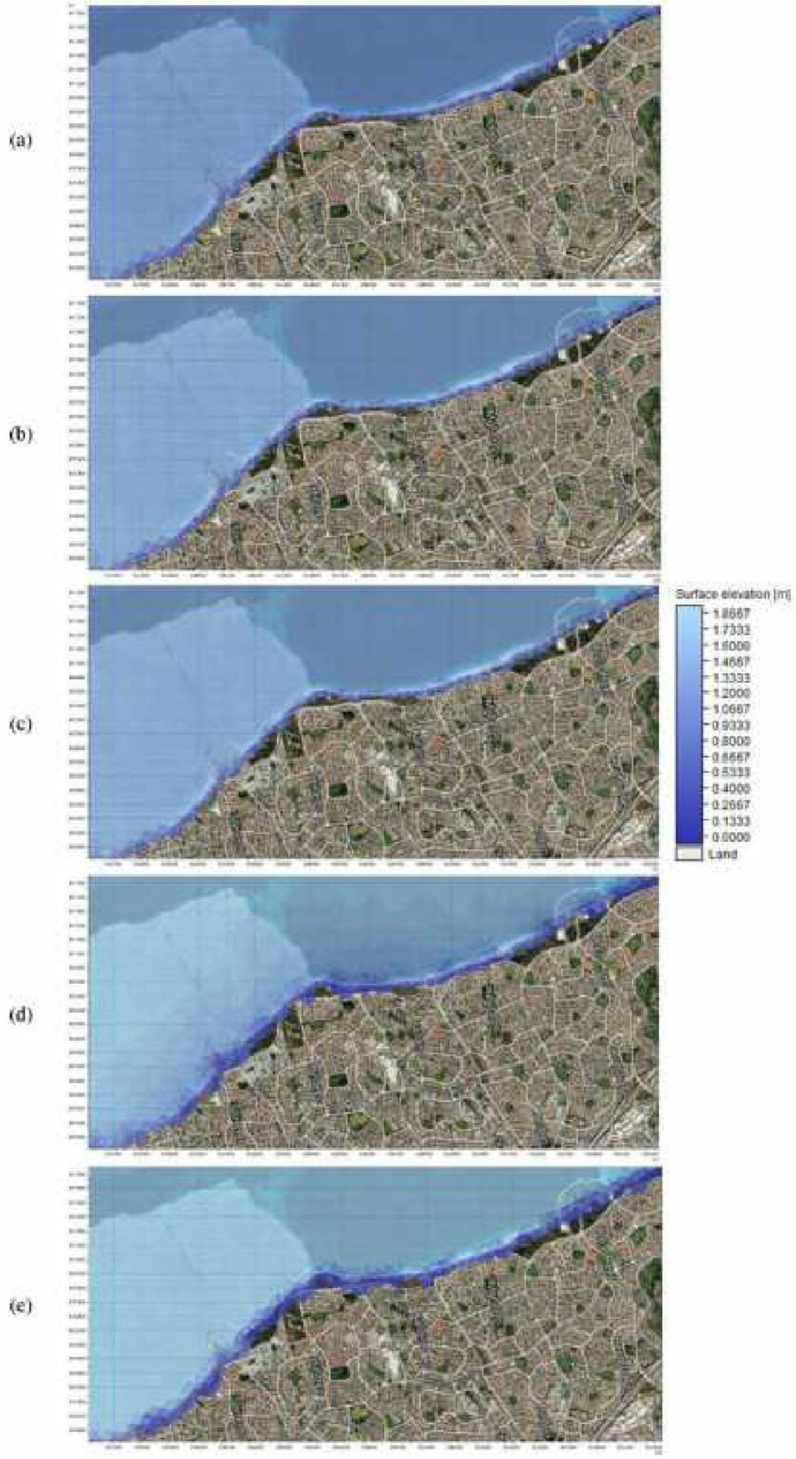

Figure 22: Flooded Footprint due to extreme Wave Events blowing from direction 270° with SLR RCP/ SSP 8.5 LC for Mullaloo, Perth (a) Hs for 1-year R.P, (b) Hs for 5-year R.P, (c) Hs for 20-year R.P, (d) Hs for 50-year R.P, (e) Hs for 100-year R.P

6. Conclusions

The research utilized an elaborate numerical model system to assess the repercussions of a warming planet on offshore wave dynamics and coastal flooding of Perth, Australia. Simulation of 75 possible future situations was performed by integrating 45-year hindcast wave data, IPCC AR6 sea-level rise scenarios, and high-resolution coastal topography using DHI MIKE 21 Spectral Wave (SW) and Hydrodynamic (HD) models. The findings indicate that significant wave heights in three major swell directions (180°, 225°, and 270°) have grown, with even more than 9.2 m extreme values under high- emissions

(RCP/ SSP 8.5 LC) and long-term sea-level rise conditions. The storm surge extent and inland penetration for the two selected urban beaches-Fremantle and Mullaloo, flooded, to a greater extent and farther inland respectively, under deluge from climate change drivers, particularly during 100-year return period events. It is expected that the coastal flooded area shall exceed ninety-seven km2 due to the extreme wave events for RCP/ SSP 8.5 LC.

In line with this, the research reinforces the utility of scenario-based numerical models in assessing coastal hazards providing practical resources to replicate complex oceanographic reactions to human induced climate change. This evidence fits in with and develops the larger academic talk on climate adaptation and marine hazard preparedness. The output of this work is the generation of very specific and local risk assessments that are necessary for coastal planning and resilience at the level of infrastructures, even in the case of oceanic fluctuations that were initially outlined by earlier works.

The study indicates that without taking measures to adapt to climate change, the future coastal inundation events can greatly influence the living conditions of the coastal communities in Perth. The demonstrated numerical modelling framework is a transferable tool that can be easily utilized for other coastal areas that are at risk, thus letting local governments and policymakers foresee and react to changing marine hazards and climate change.

7. Appendix

Appendix (1): Characteristics of Hs and SLR, and Static Water Level (SWL) for different scenarios of return periods.

Table 1. Characteristics of Hs and SLR, and Static Water Level (SWL) for 1-year R. P Scenarios

Scenario(s)	*Hs (m)*	*Tp (s)*	*SLR (m)*	*SWL (m)*
Scenario 1 Direction 180° SLR RCP/ SSP 2.6 MC 1-year R. P	3.02	13.81	0.011	1.191
Scenario 2 Direction 225° SLR RCP/ SSP 2.6 MC 1-year R. P	6.52	15.26	0.011	1.191
Scenario 3 Direction 270° SLR RCP/ SSP 2.6 MC 1-year R. P	7.00	15.40	0.011	1.191
Scenario 4 Direction 180° SLR RCP/ SSP 4.5 MC 1-year R. P	3.02	13.81	0.015	1.195
Scenario 5 Direction 225° SLR RCP/ SSP 4.5 MC 1-year R. P	6.52	15.26	0.015	1.195
Scenario 6 Direction 270° SLR RCP/ SSP 4.5 MC 1-year R. P	7.00	15.40	0.015	1.195
Scenario 7 Direction 180° SLR RCP/ SSP 7.0 MC 1-year R. P	3.02	13.81	0.021	1.201
Scenario 8 Direction 225° SLR RCP/ SSP 7.0 MC 1-year R. P	6.52	15.26	0.021	1.201
Scenario 9 Direction 270° SLR RCP/ SSP 7.0 MC 1-year R. P	7.00	15.40	0.021	1.201
Scenario 10 Direction 180° SLR RCP/ SSP 8.5 MC 1-year R. P	3.02	13.81	0.023	1.203
Scenario 11 Direction 225° SLR RCP/ SSP 8.5 MC 1-year R. P	6.52	15.26	0.023	1.203
Scenario 12 Direction 270° SLR RCP/ SSP 8.5 MC 1-year R. P	7.00	15.40	0.023	1.203
Scenario 13 Direction 180° SLR RCP/ SSP 8.5 LC 1-year R. P	3.02	13.81	0.063	1.243
Scenario 14 Direction 225° SLR RCP/ SSP 8.5 LC 1-year R. P	6.52	15.26	0.063	1.243
Scenario 15 Direction 270° SLR RCP/ SSP 8.5 LC 1-year R. P	7.00	15.40	0.063	1.243

Table 2. Characteristics of Hs and SLR, and Static Water Level (SWL) for 5-year R. P Scenarios

Scenario(s)	*Hs (m)*	*Tp (s)*	*SLR (m)*	*SWL (m)*
Scenario 16 Direction 180° SLR RCP/ SSP 2.6 MC 5 years R. P	3.42	14.03	0.055	1.235
Scenario 17 Direction 225° SLR RCP/ SSP 2.6 MC 5 years R. P	7.40	15.51	0.055	1.235
Scenario 18 Direction 270° SLR RCP/ SSP 2.6 MC 5 years R. P	7.75	15.61	0.055	1.235
Scenario 19 Direction 180° SLR RCP/ SSP 4.5 MC 5 years R. P	3.42	14.03	0.075	1.255
Scenario 20 Direction 225° SLR RCP/ SSP 4.5 MC 5 years R. P	7.40	15.51	0.075	1.255
Scenario 21 Direction 270° SLR RCP/ SSP 4.5 MC 5 years R. P	7.75	15.61	0.075	1.255
Scenario 22 Direction 180° SLR RCP/ SSP 7.0 MC 5 years R. P	3.42	14.03	0.105	1.285
Scenario 23 Direction 225° SLR RCP/ SSP 7.0 MC 5 years R. P	7.40	15.51	0.105	1.285
Scenario 24 Direction 270° SLR RCP/ SSP 7.0 MC 5 years R. P	7.75	15.61	0.105	1.285
Scenario 25 Direction 180° SLR RCP/ SSP 8.5 MC 5 years R. P	3.42	14.03	0.115	1.295
Scenario 26 Direction 225° SLR RCP/ SSP 8.5 MC 5 years R. P	7.40	15.51	0.115	1.295
Scenario 27 Direction 270° SLR RCP/ SSP 8.5 MC 5 years R. P	7.75	15.61	0.115	1.295
Scenario 28 Direction 180° SLR RCP/ SSP 8.5 LC 5 years R. P	3.42	14.03	0.315	1.495
Scenario 29 Direction 225° SLR RCP/ SSP 8.5 LC 5 years R. P	7.40	15.51	0.315	1.495
Scenario 30 Direction 270° SLR RCP/ SSP 8.5 LC 5 years R. P	7.75	15.61	0.315	1.495

Table 3. Characteristics of Hs and SLR, and StaticWater Level (SWL) for 20-year R. P Scenarios

Scenario(s)	*Hs (m)*	*Tp (s)*	*SLR (m)*	*SWL (m)*
Scenario 31 Direction 180° SLR RCP/ SSP 2.6 MC 20 years R. P	3.65	14.15	0.16	1.34
Scenario 32 Direction 225° SLR RCP/ SSP 2.6 MC 20 years R. P	8.00	15.67	0.16	1.34
Scenario 33 Direction 270° SLR RCP/ SSP 2.6 MC 20 years R. P	8.45	15.78	0.16	1.34
Scenario 34 Direction 180° SLR RCP/ SSP 4.5 MC 20 years R. P	3.65	14.15	0.18	1.36
Scenario 35 Direction 225° SLR RCP/ SSP 4.5 MC 20 years R. P	8.00	15.67	0.18	1.36
Scenario 36 Direction 270° SLR RCP/ SSP 4.5 MC 20 years R. P	8.45	15.78	0.18	1.36
Scenario 37 Direction 180° SLR RCP/ SSP 7.0 MC 20 years R. P	3.65	14.15	0.19	1.37
Scenario 38 Direction 225° SLR RCP/ SSP 7.0 MC 20 years R. P	8.00	15.67	0.19	1.37
Scenario 39 Direction 270° SLR RCP/ SSP 7.0 MC 20 years R. P	8.45	15.78	0.19	1.37
Scenario 40 Direction 180° SLR RCP/ SSP 8.5 MC 20 years R. P	3.65	14.15	0.22	1.4
Scenario 41 Direction 225° SLR RCP/ SSP 8.5 MC 20 years R. P	8.00	15.67	0.22	1.4
Scenario 42 Direction 270° SLR RCP/ SSP 8.5 MC 20 years R. P	8.45	15.78	0.22	1.4
Scenario 43 Direction 180° SLR RCP/ SSP 8.5 LC 20 years R. P	3.65	14.15	0.36	1.54
Scenario 44 Direction 225° SLR RCP/ SSP 8.5 LC 20 years R. P	8.00	15.67	0.36	1.54
Scenario 45 Direction 270° SLR RCP/ SSP 8.5 LC 20 years R. P	8.45	15.78	0.36	1.54

Table 4. Characteristics of Hs and SLR, and Static Water Level (SWL) for 50-year R. P Scenarios

Scenario(s)	*Hs (m)*	*Tp (s)*	*SLR (m)*	*SWL (m)*
Scenario 46 Direction 180° SLR RCP/ SSP 2.6 MC 50 years R. P	3.85	14.25	0.46	1.64
Scenario 47 Direction 225° SLR RCP/ SSP 2.6 MC 50 years R. P	8.40	15.77	0.46	1.64
Scenario 48 Direction 270° SLR RCP/ SSP 2.6 MC 50 years R. P	8.85	15.88	0.46	1.64
Scenario 49 Direction 180° SLR RCP/ SSP 4.5 MC 50 years R. P	3.85	14.25	0.55	1.73
Scenario 50 Direction 225° SLR RCP/ SSP 4.5 MC 50 years R. P	8.40	15.77	0.55	1.73
Scenario 51 Direction 270° SLR RCP/ SSP 4.5 MC 50 years R. P	8.85	15.88	0.55	1.73
Scenario 52 Direction 180° SLR RCP/ SSP 7.0 MC 50 years R. P	3.85	14.25	0.61	1.79
Scenario 53 Direction 225° SLR RCP/ SSP 7.0 MC 50 years R. P	8.40	15.77	0.61	1.79
Scenario 54 Direction 270° SLR RCP/ SSP 7.0 MC 50 years R. P	8.85	15.88	0.61	1.79
Scenario 55 Direction 180° SLR RCP/ SSP 8.5 MC 50 years R. P	3.85	14.25	0.7	1.88
Scenario 56 Direction 225° SLR RCP/ SSP 8.5 MC 50 years R. P	8.40	15.77	0.7	1.88
Scenario 57 Direction 270° SLR RCP/ SSP 8.5 MC 50 years R. P	8.85	15.88	0.7	1.88
Scenario 58 Direction 180° SLR RCP/ SSP 8.5 LC 50 years R. P	3.85	14.25	1.26	2.44
Scenario 59 Direction 225° SLR RCP/ SSP 8.5 LC 50 years R. P	8.40	15.77	1.26	2.44
Scenario 60 Direction 270° SLR RCP/ SSP 8.5 LC 50 years R. P	8.85	15.88	1.26	2.44

Table 5. Characteristics of Hs and SLR, and Static Water Level (SWL) for 100-year R. P Scenarios

Scenario(s)	*Hs (m)*	*Tp (s)*	*SLR (m)*	*SWL (m)*
Scenario 61 Direction 180° SLR RCP/ SSP 2.6 MC 100 years R. P	4.02	14.33	1.09	2.27
Scenario 62 Direction 225° SLR RCP/ SSP 2.6 MC 100 years R. P	8.70	15.84	1.09	2.27
Scenario 63 Direction 270° SLR RCP/ SSP 2.6 MC 100 years R. P	9.20	15.96	1.09	2.27
Scenario 64 Direction 180° SLR RCP/ SSP 4.5 MC 100 years R. P	4.02	14.33	1.32	2.5
Scenario 65 Direction 225° SLR RCP/ SSP 4.5 MC 100 years R. P	8.70	15.84	1.32	2.5
Scenario 66 Direction 270° SLR RCP/ SSP 4.5 MC 100 years R. P	9.20	15.96	1.32	2.5
Scenario 67 Direction 180° SLR RCP/ SSP 7.0 MC 100 years R. P	4.02	14.33	1.64	2.82
Scenario 68 Direction 225° SLR RCP/ SSP 7.0 MC 100 years R. P	8.70	15.84	1.64	2.82
Scenario 69 Direction 270° SLR RCP/ SSP 7.0 MC 100 years R. P	9.20	15.96	1.64	2.82
Scenario 70 Direction 180° SLR RCP/ SSP 8.5 MC 100 years R. P	4.02	14.33	1.87	3.05
Scenario 71 Direction 225° SLR RCP/ SSP 8.5 MC 100 years R. P	8.70	15.84	1.87	3.05
Scenario 72 Direction 270° SLR RCP/ SSP 8.5 MC 100 years R. P	9.20	15.96	1.87	3.05
Scenario 73 Direction 180° SLR RCP/ SSP 8.5 LC 100 years R. P	4.02	14.33	4	5.18
Scenario 74 Direction 225° SLR RCP/ SSP 8.5 LC 100 years R. P	8.70	15.84	4	5.18
Scenario 75 Direction 270° SLR RCP/ SSP 8.5 LC 100 years R. P	9.20	15.96	4	5.18

DECLARATION OF GENERATIVE AI AND AI-ASSISTED TECHNOLOGIES:

During the preparation of this work, the author(s) used Scopus AI in order to define the main related articles that cover the topic as a part of the systematic literature search conducted. After using this tool/service, the authors reviewed and edited the content as necessary and took full responsibility for the content of the publication.

8. REFERENCES

[1] Australian Department of Climate Change, Climate change risks to Australia's coast: a first pass national assessment. Canberra: Australian Dept. of Climate Change, 2009.

[2] S. Flay and J. Nott, "Effect of ENSO on Queensland seasonal landfalling tropical cyclone activity," Int. J. Climatol., vol. 27, no. 10, pp. 1327-1334, 2007.

[3] A. B. Pezza, T. Durrant, I. Simmonds, and I. Smith, "Southern Hemisphere Synoptic Behavior in Extreme Phases of SAM, ENSO, Sea Ice Extent, and Southern Australia Rainfall," Journal of Climate, vol. 21, no. 21, pp. 5566-5584, Nov. 2008.

[4] W. Wu and M. Leonard, "Impact of ENSO on dependence between extreme rainfall and storm surge," Environ.Res.Lett., vol. 14, no. 12, 2019.

[5] B. S. Hague, D. A. Jones, D. Jakob, S. McGregor, and R. Reef, "Australian Coastal Flooding Trends and Forcing Factors," Earth's Future, vol. 10, no. 2, p. e2021EF002483, Feb. 2022.

[6] M. Meinshausen, S. J. Smith, K. Calvin, J. S. Daniel, M. L. T. Kainuma, J.-F. Lamarque, K. Matsumoto, S. A. Montzka, S. C. B. Raper, K. Riahi, A. Thomson, G. J. M. Velders, and D. P. P. Van Vuuren, "The RCP greenhouse gas concentrations and their extensions from 1765 to 2300," Climatic Change, vol. 109, no. 1–2, pp. 213–241, Nov. 2011.

[7] Intergovernmental Panel On Climate Change, Climate Change and Land: IPCC Special Report on Climate Change, Desertification, Land Degradation, Sustainable Land Management, Food Security, and Greenhouse Gas Fluxes in Terrestrial Ecosystems, 1st ed. Cambridge University Press, 2022.

[8] Intergovernmental Panel on Climate Change, Ed., Climate change 2022: impacts, adaptation and vulnerability: Working Group II contribution to the Sixth Assessment Report of the Intergovernmental Panel on Climate Change. Cambridge: Cambridge University Press, 2023.

[9] Intergovernmental Panel On Climate Change (Ipcc), Climate Change 2021 – The Physical Science Basis: Working Group I Contribution to the Sixth Assessment Report of the Intergovernmental Panel on Climate Change, 1st ed. Cambridge University Press, 2023.

[10] M. Prakash, R. Cohen, J. Hilton, and S. H. Khan, "An evidence based approach to evaluating flood
adaptation effectiveness including climate change considerations for coastal cities: City of Port Phillip, Victoria, Australia," J Flood Risk Management, vol. 13, no. S1, p. e12556, Jan. 2020.

[11] K. McInnes, J. Church, D. Monselesan, J. Hunter, J. O'Grady, I. Haigh, and X. Zhang,
"Information for Australian impact and adaptation planning in response to sea-level rise," AMOJ, vol. 65, no. 1, pp. 127–149, Mar. 2015.

[12] X. Zhang, J. A. Church, D. Monselesan, and K. L. McInnes, "Sea level projections for the
Australian region in the 21st century," Geophysical Research Letters, vol. 44, no. 16, pp. 8481– 8491, Aug. 2017.

[13] F. Li, L. Roncevich, C. Bicknell, R. Lowry, and K. Ilich, "Interannual variability and trends of
storminess, Perth, 1994-2008," J. Coast. Res., vol. 27, no. 4, pp. 738–745, 2011.

[14] DHI, "MIKE 21 Spectral Waves FM," DHI, The Netherlands, User Guide, 2017.

[15] DHI, "MIKE ZERO EVA," DHI, The Netherlands, User Guide MIKE ZERO Extreme Value
Anaysis, 2019.

[16] M. Abouelnasr, "Future Proof Infrastructure for Port-City: Case Study for the Sustainability of
Suez Canal Entrance Groins against Future Extreme Wave Conditions," MARLOG 12 Conference, vol. 12, no. 1, p. 174, 2023.

[17] M. Abouelnasr and A. Elselmy, "Medicanes and its Metrological Effects in the Mediterranean Sea:
Case Study of Medicane Ianos," MARLOG 13 Conference, vol. 13, no. 1, p. 273, 2024.

[18] J. Su, J. Murawski, J. W. Nielsen, and K. S. Madsen, "Coinciding storm surge and wave setup: A regional assessment of sea level rise impact," Ocean Engineering, vol. 305, p. 117885, Aug. 2024.

[19] L. W. Broadbridge and B. N. Hanstrum, "The relationship between tropical cyclones near Western
Australia and the Southern Oscillation Index," Aust. Meteorol. Mag., vol. 47, no. 3, pp. 183–189, 1998.
[20] F. Li, C. Bicknell, R. Lowry, and Y. Li, "A comparison of extreme wave analysis methods with
1994-2010 offshore Perth dataset," Coast. Eng., vol. 69, pp. 1–11, 2012.
[21] X. Sun, B. Renard, M. Lang, and M. Thyer, "Modelling the non-stationary, asymmetric impact of
ENSO on seasonal rainfall totals and daily rainfall extremes," in Proc. Hydrol. Water Resour. Symp., HWRS, 2012, pp. 1264–1272.
[22] D. Waters, B. Cechet, and C. Arthur, "Role of exposure in projected residential building cyclone
risk for the Australian region," IOP Conf. Ser.: Earth Environ. Sci., vol. 11, p. 012022, Aug. 2010.
[23] J. Haig, "Investigating long-term, high-resolution records of climate and extreme events in the
southeast Indian and southwest Pacific oceans using the δ18O of stalagmites," 2015.
[24] X. Pan and A. Rahman, "Comparison of annual maximum and peaks-over-threshold methods with
automated threshold selection in flood frequency analysis: a case study for Australia," Nat. Hazards, vol. 111, no. 2, pp. 1219–1244, 2022.
[25] D. Taylor, J. Aldridge, J. Dent, and J. Churchill, "National scale mutli-hazard model platform for
extreme cyclone impacts on coasts and infrastructure," in Proc Coastal Eng Conf, 2018, vol. 36, no. 2018.
[26] I. L. Turner, C. K. Leaman, M. D. Harley, M. C. Thran, D. R. David, K. D. Splinter, N. Matheen,
J. E. Hansen, M. V. W. Cuttler, D. J. M. Greenslade, S. Zieger, and R. J. Lowe, "A framework for national-scale coastal storm hazards early warning," Coastal Engineering, vol. 192, p. 104571, Sept. 2024.
[27] C.-H. Wang, "Bias and variance reduction of high return levels for extreme hazard modelling,"
Nat. Hazards, vol. 120, no. 3, pp. 2461–2478, 2024.
[28] A. J. Lemm, B. J. Hegge, and G. Masselink, "Offshore wave climate, Perth (Western Australia),
1994-96," Mar. Freshw. Res., vol. 50, no. 2, pp. 95–102, 1999.
[29] G. Masselink, "Sea breeze activity and its effect on coastal processes near Perth, Western
Australia," J. R. Soc. West. Aust., vol. 79, no. 3, pp. 199–205, 1996.
[30] J. McDonald, "Hot in the city: Planning for climate change impacts in urban Australia," in Four
Degrees of Global Warming: Australia in a Hot World, Taylor and Francis, 2013, pp. 172–189.
[31] F. Zheng, M. Leonard, and S. Westra, "Application of the design variable method to estimate
coastal flood risk," J Flood Risk Management, vol. 10, no. 4, pp. 522–534, Dec. 2017.
[32] N. Mori, T. Shimura, K. Yoshida, R. Mizuta, Y. Okada, M. Fujita, T. Khujanazarov, and E.

Nakakita, "Future changes in extreme storm surges based on mega-ensemble projection using 60- km resolution atmospheric global circulation model," Coastal Engineering Journal, vol. 61, no. 3, pp. 295–307, July 2019.
[33] R. J. Lowe, M. V. W. Cuttler, and J. E. Hansen, "Climatic Drivers of Extreme Sea Level Events
Along the Coastline of Western Australia," Earth's Future, vol. 9, no. 4, p. e2020EF001620, Apr. 2021.
[34] J. A. Church, J. Hunter, K. L. McInnes, and N. White, "Sea-level rise around the Australian
coastline and the changing frequency of extreme sea-level events," Jan. 2006.
[35] K. Kumbier, R. C. Carvalho, and C. D. Woodroffe, "Modelling Hydrodynamic Impacts of Sea-
Level Rise on Wave-Dominated Australian Estuaries with Differing Geomorphology," JMSE, vol. 6, no. 2, p. 66, June 2018.
[36] W. Steffen, L. Hughes, and J. Hunter, Counting the cost: climate change and coastal flooding.
Surry Hills, N.S.W.: Climate Council of Australia, 2014.
[37] M. Abouelnasr, "Raw Dataset for offshore Hindcast Waves data for 17 Ports along the Mediterranean Sea." Mendeley, 03-Jan-2023.
[38] C3S, "ERA5 hourly data on single levels from 1940 to present." [object Object], 2018.
[39] S. Bell, A. Dowdy, S. Chand, and C.-H. Su, "Occurrence and trends of historical tropical cyclone
rainfall on near-coastal regions of Australia," J. South. Hemisph. Earth Syst. Sci., vol. 74, no. 2, July 2024.
[40] S. S. Bell, A. J. Dowdy, H. A. Ramsay, S. S. Chand, C.-H. Su, and H. Ye, "Using historical tropical
cyclone climate datasets to examine wind speed recurrence for coastal Australia," Sci Rep, vol. 12, no. 1, July 2022.
[41] J. Olauson, "ERA5: The new champion of wind power modelling?," Renewable Energy, vol. 126,
pp. 322–331, Oct. 2018.
[42] GEBCO Bathymetric Compilation Group 2025, "The GEBCO_2025 Grid - a continuous terrain
model for oceans and land at 15 arc-second intervals." NERC EDS British Oceanographic Data Centre NOC, 2025.
[43] B. Tozer, D. T. Sandwell, W. H. F. Smith, C. Olson, J. R. Beale, and P. Wessel, "Global
Bathymetry and Topography at 15 Arc Sec: SRTM15+," Earth and Space Science, vol. 6, no. 10, pp. 1847–1864, Oct. 2019.
[44] NASA JPL, "NASA SRTM Image Mosaic Global 1 arc second V001." NASA Land Processes
Distributed Active Archive Center, 2020.
[45] R. Parums and M. Spinoccia, "50m Multibeam Dataset of Australia 2018." Commonwealth of
Australia (Geoscience Australia), 2019.
[46] O. Wilson, M. Spinoccia, and C. Buchanan, "50m Multibeam Dataset of Australia 2012," 50m

Multibeam Dataset of Australia 2012, 2012. [Online]. Available: https://ecat.ga.gov.au/geonetwork/srv/eng/catalog.search#/metadata/73842. [Accessed: 22-May- 2024].

[47] Geoscience Australia, "Digital Elevation Model (DEM) of Australia derived from LiDAR 5 Metre
Grid." Commonwealth of Australia (Geoscience Australia), 2015.

[48] R. Bishop-Taylor, R. Nanson, S. Sagar, and L. Lymburner, "Mapping Australia's dynamic
coastline at mean sea level using three decades of Landsat imagery," Remote Sensing of Environment, vol. 267, p. 112734, Dec. 2021.

[49] U. Lebrec, V. Paumard, M. J. O'Leary, and S. C. Lang, "Towards a regional high-resolution
bathymetry of the North West Shelf of Australia based on Sentinel-2 satellite images, 3D seismic surveys and historical datasets." Geophysics and geodesy, 11-June-2021.

[50] Geoscience Australia, R. Bishop-Taylor, R. Nanson, and L. Lymburner, "Digital Earth Australia
Coastlines." Commonwealth of Australia (Geoscience Australia), 2021.

[51] R. Bishop-Taylor, R. Nanson, S. Sagar, and L. Lymburner, "Mapping Australia's dynamic
coastline at mean sea level using three decades of Landsat imagery," Remote Sensing of Environment, vol. 267, p. 112734, Dec. 2021.

[52] P. Wessel and W. H. F. Smith, "A global, self-consistent, hierarchical, high-resolution shoreline
database," J. Geophys. Res., vol. 101, no. B4, pp. 8741–8743, 2017.

[53] European Union-Copernicus Marine Service, "Global Ocean Waves Reanalysis WAVERYS."
Mercator Ocean International, 2019.

[54] S. Law-Chune, L. Aouf, A. Dalphinet, B. Levier, Y. Drillet, and M. Drevillon, "WAVERYS: a
CMEMS global wave reanalysis during the altimetry period," Ocean Dynamics, vol. 71, no. 3, pp. 357–378, Mar. 2021.

[55] European Union-Copernicus Marine Service, "Global Ocean Waves Analysis." Mercator Ocean
International, 2018.

[56] A. Lotfi and A. Dalphinet, "SYNTHESIS QUALITY OVERVIEW DOCUMENT (SQO)," 3.2, 2025.

[57] D. Lucio, J. L. Lara, A. Tomás, and I. J. Losada, "Projecting compound wave and sea-level events
at a coastal structure site under climate change," Coastal Engineering, vol. 189, p. 104490, Apr. 2024.

[58] P. Galiatsatou, C. Makris, and P. Prinos, "Optimized Reliability Based Upgrading of Rubble
Mound Breakwaters in a Changing Climate," JMSE, vol. 6, no. 3, p. 92, Aug. 2018.

[59] T. Thomas, N. Rangel-Buitrago, M. Phillips, G. Anfuso, and A. Williams, "Mesoscale
Morphological Change, Beach Rotation and Storm Climate Influences along a Macrotidal Embayed Beach," JMSE, vol. 3, no. 3, pp. 1006–1026, Sept. 2015.

[60] A. Jokiel-Rokita and S. Pią tek, "Estimation of parameters and quantiles of the Weibull
distribution," Stat Papers, vol. 65, no. 1, pp. 1–18, Feb. 2024.

[61] I. Arfa, A. González-Rosell, K. Govorukha, B. Bisselink, and M. Blanco, "Developing narratives
for policy-relevant water-energy-food-ecosystem nexus pathways: How global and European Union drivers interact," Environmental Impact Assessment Review, vol. 116, p. 108122, Jan. 2026.
[62] A. Nauels, J. Rogelj, C.-F. Schleussner, M. Meinshausen, and M. Mengel, "Linking sea level rise
and socioeconomic indicators under the Shared Socioeconomic Pathways," Environ. Res. Lett., vol. 12, no. 11, p. 114002, Nov. 2017.
[63] A. Fekry and A. Hamouda, "Hydrographic Surveys as an Art of Delineating the Impact of Climate
Change on the Coastal Environment," MARLOG 11 Conference, vol. 11, no. 1, p. 99, 2022.
[64] K. L. McInnes, C. J. White, I. D. Haigh, M. A. Hemer, R. K. Hoeke, N. J. Holbrook, A. S. Kiem,
E. C. J. Oliver, R. Ranasinghe, K. J. E. Walsh, S. Westra, and R. Cox, "Natural hazards in Australia: sea level and coastal extremes," Climatic Change, vol. 139, no. 1, pp. 69–83, Nov. 2016.
[65] K. McInnes, J. Church, D. Monselesan, J. Hunter, J. O'Grady, I. Haigh, and X. Zhang,
"Information for Australian impact and adaptation planning in response to sea-level rise," AMOJ, vol. 65, no. 1, pp. 127–149, Mar. 2015.
[66] J. Van Alphen, M. Haasnoot, and F. Diermanse, "Uncertain Accelerated Sea-Level Rise, Potential
Consequences, and Adaptive Strategies in The Netherlands," Water, vol. 14, no. 10, p. 1527, May 2022.
[67] W. E. Featherstone, N. T. Penna, M. S. Filmer, and S. D. P. Williams, "Nonlinear subsidence at
Fremantle, a long-recording tide gauge in the Southern Hemisphere," JGR Oceans, vol. 120, no. 10, pp. 7004–7014, Oct. 2015.
[68] M. S. Filmer, S. D. P. Williams, C. W. Hughes, G. Wöppelmann, W. E. Featherstone, P. L.
Woodworth, and A. L. Parker, "An experiment to test satellite radar interferometry-observed geodetic ties to remotely monitor vertical land motion at tide gauges," Global and Planetary Change, vol. 185, p. 103084, Jan. 2020.
[69] D. P. Van Vuuren, J. Edmonds, M. Kainuma, K. Riahi, A. Thomson, K. Hibbard, G. C. Hurtt, T.
Kram, V. Krey, J.-F. Lamarque, T. Masui, M. Meinshausen, N. Nakicenovic, S. J. Smith, and S. K. Rose, "The representative concentration pathways: an overview," Climatic Change, vol. 109, no. 1–2, pp. 5–31, Nov. 2011.
[70] B. J. Van Ruijven, M. A. Levy, A. Agrawal, F. Biermann, J. Birkmann, T. R. Carter, K. L. Ebi,
M. Garschagen, B. Jones, R. Jones, E. Kemp-Benedict, M. Kok, K. Kok, M. C. Lemos, P. L. Lucas, B. Orlove, S. Pachauri, T. M. Parris, A. Patwardhan, A. Petersen, B. L. Preston, J. Ribot, D. S. Rothman, and V. J. Schweizer, "Enhancing the relevance of Shared Socioeconomic Pathways for climate change impacts, adaptation and vulnerability research," Climatic Change, vol. 122, no. 3, pp. 481–494, Feb. 2014.
[71] K. Liu, R. Wang, S. K.C., A. Goujon, G. Kiesewetter, and R. Hoekstra, "Integrating air pollution- health feedback into climate projections: towards endogenous environmental-social links in the integrated models," Environment International, vol. 204, p. 109817, Oct. 2025.

[72] M. R. Kaloop, M. El-Diasty, J. W. Hu, and F. Zarzoura, "Hybrid Artificial Neural Networks for
Modeling Shallow-Water Bathymetry via Satellite Imagery," IEEE Trans. Geosci. Remote Sensing, vol. 60, pp. 1–11, 2022.

[73] G. J. Gorman, M. D. Piggott, M. R. Wells, C. C. Pain, and P. A. Allison, "A systematic approach
to unstructured mesh generation for ocean modelling using GMT and Terreno," Computers & Geosciences, vol. 34, no. 12, pp. 1721–1731, Dec. 2008.

[74] G. B. D. N. Vieira, A. R. Pereira, and S. Koide, "Analysis of the Influence of the Numerical Mesh
in the Hydrodynamic Modelling of Lake Paranoá Using Mike 3," RGSA, vol. 17, no. 10, p. e04050, Oct. 2023.

[75] Integrated Marine Observing System (IMOS), "IMOS Hillarys Dataset." National Collaborative Research Infrastructure Strategy (NCRIS), 2025.